Monitoring of red tides in the UAE using a qualitative satellite-based index

by

Sheikha S. Al Kitbi

A Thesis Presented to the Masdar Institute of Science and Technology in Partial Fulfillment of the Requirements for the Degree of
Master of Science in Water and Environmental Engineering

March 2015

Monitoring of red tides in the UAE using a qualitative satellite-based index

by

Sheikha S. Al Kitbi

A Thesis Presented to the Masdar Institute of Science and Technology in Partial Fulfillment of the Requirements for the Degree of
Master of Science in Water and Environmental Engineering

March 2015

AUTHOR'S DECLARATION

I understand that copyright in my thesis is transferred to Masdar Institute of Science and Technology.

Author Sheikha

RESEARCH SUPERVISORY COMMITTEE MEMBERS

Dr. Marouane Temimi, _____
Masdar Institute of Science and Technology

Dr. Hosni Ghedira, _____
Masdar Institute of Science and Technology

Dr. Shadi Hasan, _____
Masdar Institute of Science and Technology

Abstract

The Red Tide Index (RI) was first introduced in 2006 by Ahn and Shanmugam. RI indicates the presence of harmful algal blooms as a proxy for chlorophyll-a concentration that is used in ocean color measurements. Other variables such as suspended sediments (SSC) and dissolved organic matter (DOM) are not accounted for in the RI, as it is the case in the other standard spectral ratios algorithms. Intense proliferation of phytoplankton during bloom conditions causes an increase in light absorption in the lower green to blue wave bands and strong scattering in the green wave bands. Hence, exploiting this finding, a new red tide index (RI) is established.

This project aims to a) develop a qualitative index, commonly known as the red tide index, to monitor, detect, and identify possible areas of Harmful Algal Blooms in the UAE and b) verify the developed index using field and laboratory analysis for the characterization of sea water samples. The red tide index makes use of satellite imagery acquired in different wavelengths. The work includes the outcomes of the intensive field work that the Masdar's Ocean Color team is conducting in the Gulf region to verify the developed index. We expect that the developed index provides end-users with a reliable tool to monitor red tides in the region. The implementation of the index operationally should be straightforward as it does not require extensive data processing and atmospheric correction.

This research was supported by the Government of Abu Dhabi to help fulfill the vision of the late President Sheikh Zayed Bin Sultan Al Nahyan for sustainable development and empowerment of the UAE and humankind.

Acknowledgments

My Thesis is dedicated to a very special person to my heart “My Dad “. My Dad has passed away during my Master’s studies and this thesis is dedicated to him. His encouragement and help was the guidance to reach this level. I would not forget my lovely and beautiful mother which always prays for my success. Special thanks to my sisters and my brothers to be patient with me during these two years.

I am grateful to my Professor. Marouane Temimi, as without him this thesis would not been completed. His continuous support, patience and wise guidance were appreciated.

I also want to thank My RSC members for their advices and time

I would like to Thank Jun Zhao who stands with me from the beginning as well as Nahla Mezhoud which was generous with her time and help.

I want also to thank my friends and colleges for their ultimate support and time.

Contents

List of Tables

List of Figures

CHAPTER 1

Introduction

1.1 Problem statement

The Arabian Gulf has been subjected to Harmful Algal Blooms (HABs) regularly with major outbreaks recorded almost every year over the last decade. HABs pose serious threats to marine ecosystems, economy of coastal cities, and the safe operation of desalination plants. Since countries surrounding the Arabian Gulf depend mostly on desalination plants because it is the generator of freshwater, monitoring and prompt response to HABs outbreaks is becoming an urgent priority for environmental authorities and desalination plant operators.

During recent years, HABs have become an increasing problem in the Arabian Gulf. Indeed, HABs have various harmful effects as they cause the inability to use water for desalinization and affect the goodness of life along periods of time. HABs can impact tourism, social relationships, seafood industries, aquaculture operations, businesses as well as huge mortalities to fish population and the other sea living. On the other hand it has a great effect on the water quality which in return influences human health.

1.2 Objective of the project

The objective of this thesis is to promote a method for bloom detection using satellite imagery and assess its performance using in situ observations. This research project contributes to the development of qualitative satellite-based index to detect red tides outbreaks in the Arabian Gulf. Such effort should require detailed understanding of water properties, which includes microbiological properties (phytoplankton abundance and biodiversity) and physicochemical properties (salinity, temperature, turbidity, pH etc.) as well as red tides frequency and spatial abundant in the Arabian Gulf.

The project objectives are:

- Develop remote sensing-based system for early warning capability for HABs to support plant operators. A qualitative index, commonly known as the red tide index will be established using Moderate Resolution Imaging Spectrometer (MODIS) data.
- Provide guidance for HAB response according to the historic records of the developed red tide index.

The outcome of this research is a tool that makes use of the developed red tide index to monitor seawater quality and their change in space and time. Moreover, early detection and warning of red tide outbreaks in the Arabian Gulf can be achieved using an effective tool as remote sensing data. We expect that the developed index will provide end-users with a reliable tool to monitor red tides in the region. The implementation of the index operationally should be straightforward, as it does not require extensive data processing and atmospheric correction.

1.3 Literature review

The outbreak and development of red tides have been detected in tropical and warm-temperate waters all over the world, such as the Arabian Gulf, Sea of Oman, Arabian Sea Caribbean Sea, eastern and western Pacific Ocean, the eastern Atlantic Ocean, Indian Ocean, and Mediterranean Sea. Algal blooms caused global concern because of the risks posed to the marine environment. These risks come from plankton that may excrete toxins or by the size of its biomass. Depletion of dissolved oxygen in the water leads to the death of marine organisms where the decomposition of plankton causes bacteria multiply and spoils the water. Some shellfish feed on certain types of plankton toxic, which may affect the nervous system of the human being. An algal bloom is a problem afflicting many countries all over the world [1] like in the East China Sea (ECS), where the algal bloom is an annual phenomenon [2, 3]. Southern coastal waters of Korea also suffer from the algal blooms especially in in Masan and Jinahe bays usually appears from June to August with different developing factors [4]. Meteorological data was used to differentiate the marine environment and the circumstance linked with the lifetime of organisms causing algal blooms. For example, coastal regions of U.S especially the northeastern and northwestern U.S suffered from toxic species of the dinoflagellates of the genera *Alexandrium*, *Gymnodinium*, and *Pyrodinium and* diatoms of the genus *Pseudo-nitzschia* that cause paralytic shellfish poisoning (PSP) and amnesic shellfish poisoning (ASP) in humans because of the production of domoic acid (DA) respectively. Potentially harmful bloom species were present in the Santa Monica Bay California in America accompanied by high nitrate, silicon and phosphate concentrations [5]. This occurs after a strong upwelling or during the starting of seasonal stratification. At least one species from Pseudo-nitzschia spp., P. micans *and* L. polyedrum were detected in

each sample during the 2-year-study. Moreover, impacts of HABs also reached the Pacific coast of North America, from Alaska to Mexico causing a threat to the natural resources and coastal economic which specify a need for systematic economic assessments [6]. In late 2008, catastrophic red tides hit the Arabian Gulf, which lasted from August 2008 to August 2009. In this incident large amounts of fish were killed resulting in the loss of a huge amount of aquatic food source. Far from the effects of red tides on human health and marine organisms, another aspect is the influence on the desalination plant that is the main source of potable water in the UAE. High biomass HABs have affected a critical compound of seawater desalination, which is the seawater intake by clogging of intake filters which caused the closure of desalination plant during the Algal bloom episode in the Arabian Gulf in 2008 and 2009 [7]. Biofouling due to dissolved organic materials damaged reverse osmosis (RO) membranes.

Lately, increases in frequency, amount and geographic distribution of Harmful Algal Blooms (HABs) all over the world have been observed by scientists The Arabian Gulf has been also subjected to HABs regularly with outbreaks recorded almost every year over the last decade [8]. Different monitoring techniques have been integrated to detect and track algal blooms outbreaks, including remote sensing data based on satellite observations, using optical properties, spectral ratio discrimination, satellite chlorophyll anomaly, fluorescence line height (FLH) algorithm, climatological data analysis, as well as in situ surveys [9]. Several studies of remote sensing technology applications have been performed to study algal blooms phenomena over the last decades. In a case study of the 2008 red tide event, dominated by *Cochlodinium polykriloides*, that was observed on the east coast of the UAE, combined satellite imagery with numerical model simulation were used to monitor and asses the HABs

formation. This study gives an overview on the initiation and the nutrient sources that help the formation of such blooms as well as the maintenance mechanisms [10]. More studies emphasizing in the same issue for example, a study using MODIS Sensor Data detect a red tide event included about 140,000 km2 of the Arabian Gulf and total area of Strait of Hormuz and last for 9 months. Previous studies revealed that the seawater temperature drop, water circulation and the adverse environmental pollutions caused by industrial and urban sewages was the main red tide causes [11]. Other local meteorological and oceanographic factors can play a role in the formation of red tides in the Arabian Gulf, including vertical stratification, precipitation, and aeolian dust transport, which have been observed based on the seasonal and interannual variability of remotely sensed chlorophyll. It was noticed that the Gulf surface has exposure to low precipitation periods between 2000 and 2008, which encounters high dust level followed by blooms [12].

The spatial and temporal variability of HABs was successfully achieved by a new method developed in 2006 named the red tide index (RI) [9]. The result showed a consistent manner with the in situ measurements which make it an effective way of monitoring algal blooms [9]. Moving away from Arabian Gulf, Southwestern Florida Coastal water was also subjected to harmful algal blooms. Another study also used the red tide index (RI) algorithm that was developed previously in 2006 instead of traditional methods to detect Florida's algal blooms. RI was developed using ocean color data from the Seaviewing Wide Field-of-view Sensor (SeaWiFS). This new method reveals a promising future for the red tide monitoring approach [13]. Current global algorithms such as OC3 and OC4v4 results showed overestimated chlorophyll a concentration for open ocean waters and regions with chlorophyll a concentration < 0.5 mg m−3 as the presence of other suspended sediments and dissolved substances.

A new bio-optical algorithm was developed using five different data sets, SeaWiFS/MODIS matchups and MODIS/Aqua imagery from different and then was evaluated statistically with the previous algorithms. Chlorophyll assessment showed better result with the new algorithm [14]. The previous site studies and many others emphasized the importance of the satellite method over the traditions means of chlorophyll a retrievals.

The advantages of remote sensing are large-scale, real-time, cost-effective, and long-term monitoring. Furthermore, satellite observations can reach areas unreachable for human beings. It is very important to understand HABs oceanographic mechanisms and set planned strategies to ensure a powerful monitoring and detecting of HABs as well as understanding of phytoplankton proprieties in the Arabian Gulf [10]. Dealing with remote sensing data needs a strong background over the satellite manipulation techniques.

Remote sensing disadvantages arise from the large errors in the satellite Chl retrieval such as atmospheric correction error and dust which reduce the ability of satellite to detect the areas of HABs.

1.4 Phytoplankton

1.4.1 Definition

Phytoplankton are free-floating microscopic organisms that live in the ocean, composed of both eukaryotic (microalgae) and prokaryotic (cyanobacteria) species. The name of phytoplankton is originally come from the Greek words *phyto* (plant) and *plankton* (wanderer or drifter). Phytoplankton obtains energy through the process of photosynthesis. Their growth depends on the availability of sunlight, nutrients (Phosphorous, nitrogen, silicon, iron etc.) and other physical parameters of the water

(salinity, temperature, pH etc.). They inhabit the upper sunlit layer (euphotic zone) of almost all oceans and fresh water bodies around the world. During the photosynthesis process, phytoplankton consumes carbon dioxide and produces oxygen. That makes the ocean a type of carbon sink, which prevents carbon dioxide accumulation in the atmosphere [15]. The photosynthesis process production of organic materials constitutes the first link (the primary source of nutrition) of the oceanic food chain that reaches through all trophic levels (Fig.1). That makes them an important component.

The most important groups of phytoplankton include the cyanobacteria (blue-green algae), diatoms, and dinoflagellates which have characteristic shapes as shown in figure 2. The astonishing diversity of phytoplankton is visible only under a microscope.

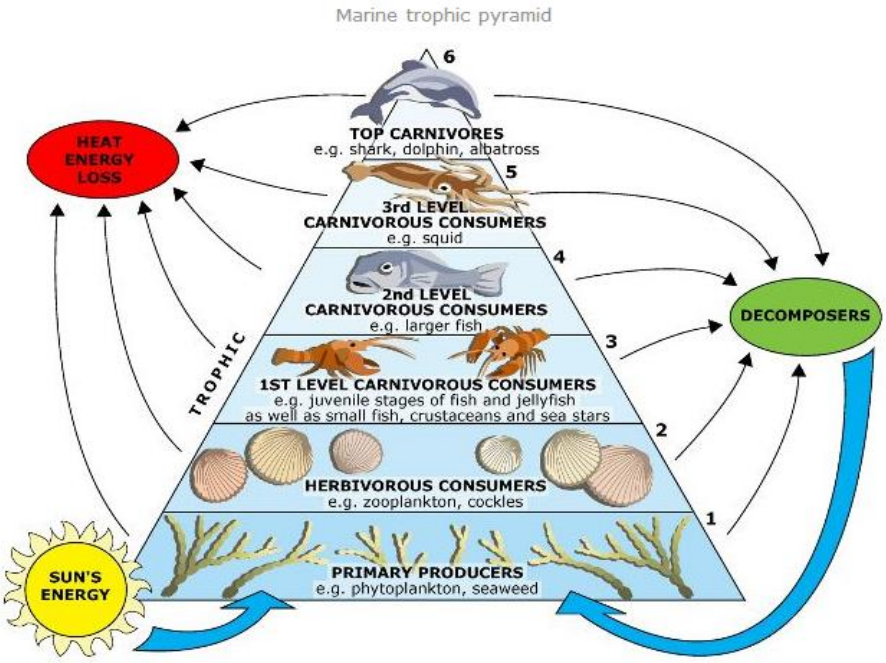

Figure 1: The base marine trophic pyramid where phytoplankton is the primary producer (Source: http://sciencelearn.org.nz/Contexts/Life-in-theSea/Sci-Media/Images/Marine-trophic-pyramid)

1.4.2 Chlorophyll

Chlorophyll is a green pigment found in almost all plants, algae, and cyanobacteria. Chlorophyll-*a* (*Chl-a*) is the most common specific form of chlorophyll, and is present in all photosynthetic organisms. Other accessory pigments such as chlorophyll b and c may occur in phytoplankton (Table 1). The presence or absence of such various pigments is used among other features, to separate the major algal groups. The amount of *Chl- a* in phytoplankton constitutes generally about 1 to 2 % of the dry weight. As potential indicators of maximum photosynthetic rate expressed in $\mu g.L^{-1}$ or in $mg.m^{-3}$can be used to indicate phytoplankton abundance and biomass in the water. Furthermore, as a proxy of phytoplankton biomass, can be an effective measure of trophic status of any water body. Therefore, it is commonly used to measure of water quality and thus to determine the level of pollution of water.

Extraction of chlorophyll and determining its concentration in a sample consider the most effective way to find the phytoplankton density. The quantification of chlorophyll a is easier than the algal biomass itself [16, 17].

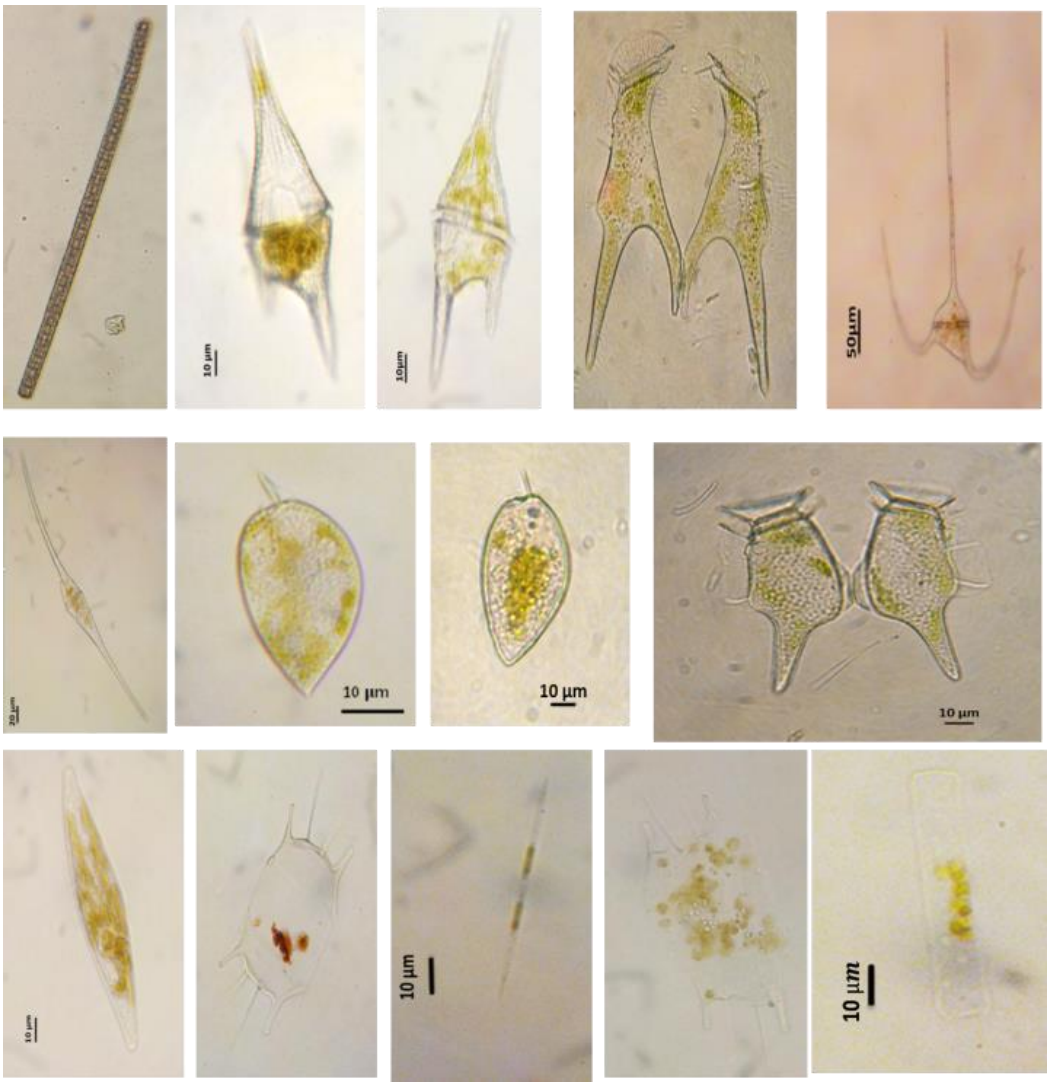

Figure 2: Light microscope micrographs of phytoplankton (a) Cyanbacteria, (b-i) Dinoflagellates, and (i-n) Diatoms. Data courtesy of Mezhoud et al. (2014).

1.4.2.1 Chlorophyll chemical structure and absorption**:**

Chlorophyll is composed of different types, including chlorophyll-a (Chl-a), Chl-b, Chl-c, and Chl-d. Chl-a exists in all photosynthesizing plants and cyanobacteria, except bacteria. Chl- *a* ($C_{55}H_{72}O_5N_4Mg$) and b ($C_{55}H_{70}O_6N_4Mg$) have a common basic structure as shown in figure 3. Chl –*b*, the second variety of chlorophyll present in green plants and green algae, differs from Chl-*a* only by local oxidation of one side chain. This side chain is –CH3 in Chl-*a* and in Ch-*b*. Chlorophyll does not absorb light equally over the visible bands. The absorption spectra of Chl-a and b are shown in figure 4. Chl-*a* does not absorb light in the green part (480-560 nm) of the spectrum

while Chl-b indicates weak absorption. The absorption characteristics of Chl-a-d are listed in Table 1. Chl-a and b demonstrate different absorption peaks with 420 and 660 nm for Chl-a and 453 and 643 nm for Chl-b in organic solvents. Chl-c present in diatoms and brown algae has absorption peaks at 445 and 625 nm in organic solvents. Chl-d peaks at 450 and 690 nm in organic solvents. The absorption peaks of these pigments differ in *in vivo* phytoplankton cells

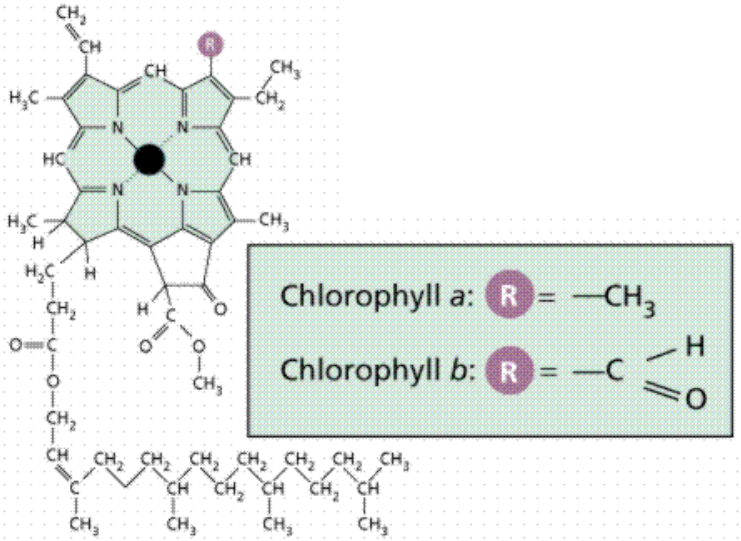

Figure 3: The molecular structure of Chl-a and –b
(Source: Purves et al., 2009).

Table 1: Characteristics absorption of Chlorophylls and occurrence (Source: Rabinowitch and Govindjee. 1970)

Type of Chlorophyll	**Characteristic absorption peaks**		**Occurrence**
	In organic solvents, nm	**In Cell, nm**	
Chl a	420, 660	435,670-680 (several forms)	All photosynthesizing plants(except bacteria)
Chl b	453, 643	480, 650	Higher plants and green algae

Chl c	445, 625	Red band at 645	Diatoms and brown algae
Chl d	450, 690	Red band at 740	Reported in some red algae

1.4.2.2 Optical features:

The hues of ocean differ from blue to brown as shown in figure 5. From outer space, satellite sensors can distinguish even slight variations in color to which our eyes are not sensitive [18]. The color of seawater depends on the scattering and absorption properties of the constituents in the water column.

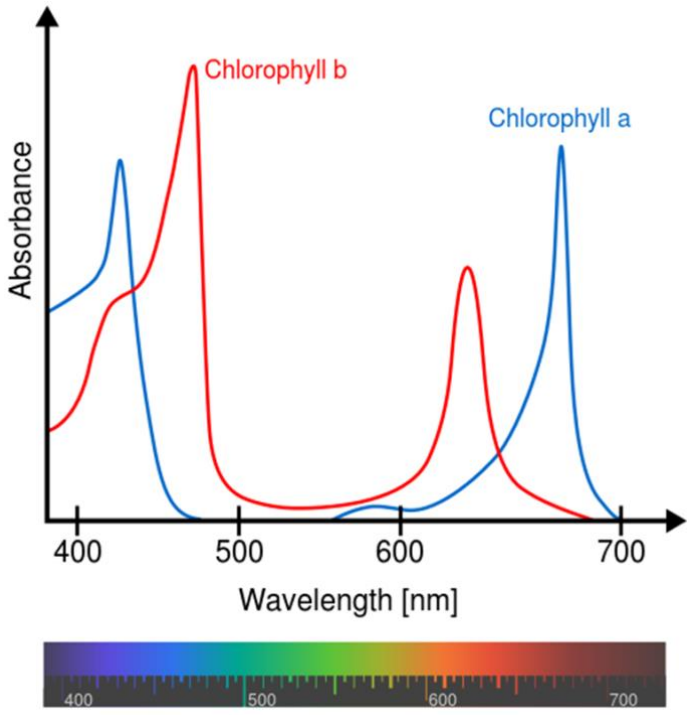

Figure 4: The absorbance spectra of free Chl-a and –b in a solvent.

Conversely, the optical properties of the seawater components can be retrieved through different algorithms by using the radiance/reflectance spectra of seawater. The optical properties of the seawater are usually estimated with a three-component model [19, 20], namely, phytoplankton, colored dissolved organic matter (CDOM) or gelbstoff, and suspended sediments. The absorption and scattering coefficients of seawaters are determined by the concentrations of these constituents.

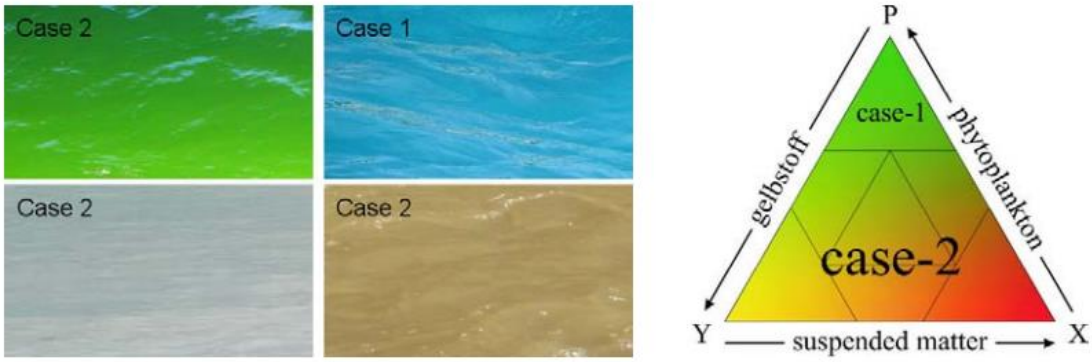

Figure 5: Examples of different colored sea areas and diagram representing the Case 1 and Case 2 waters. Case 1 waters represent the phytoplankton dominant cases, whereas Case 2 waters represent all other possible cases (Source: Sathyendranath, 2000)

Different shades of ocean color can be measured by satellites and reveals the presence of differing concentrations of phytoplankton, sediments and organic materials. high concentrations of phytoplankton in ocean will occur as certain shades, from blue-green to green, which depends on the concentration and type phytoplankton population there due to the reflectance of the green light by chlorophyll phytoplankton [18].

1.5 Harmful Algal blooms

1.5.1 Definition

During periods of optimum growth, microalgae can reach maximum concentrations in seawater. This commonly known as algal or phytoplankton blooms [21]. These

blooms are one of the natural causes of discoloration of marine and freshwater bodies throughout the world. Pigmented blooms produced by marine algae are named as “red tides”. The commonly used name for Red tides is harmful algal blooms (HABs) since the blooms sometimes colored with different than red color and are not directly associated with tides, Its known when algal bloom can be dangerous to other organisms or increase the biomass of algal toxins in the water which in return affect other organisms of the food chain [22].

The color of HABs relies on the phytoplankton species which usually ranges from blood red to orange or brown or green in daylight. (Fig.6). Approximately 300 algal species of the 5000 species of extant marine phytoplankton can form HABs. Of the more these 5,000 known species, production of toxins are linked to approximately 40 species worldwide. Due to lack of research and data about phytoplankton ecology it is very hard to reduce the harmful drawbacks of toxin blooms. [23].

Among the 300 worldwide HABs species, eight different genus (*Trichodesmium*, *Pseudo-Nitzschia*, *Thalassiothrix*, *Gonyaulax*, *Noctiluca*, *Prorocentrum*, *Amphidinium*, and *Cochlodinium*) were found to cause HABs in the Arabian Seas (Arabian Gulf, Sea of Oman and Arabian Sea) [24]. These common phytoplankton are responsible for the HABs outbreak in the Arabian Seas is summarized in Tables 1, 2 and 3.

HABs may cover hundreds of square kilometers that could be traced by satellite images [25] as shown in figure 7.

Figure 6: Colored HABs commonly occurring in Omani waters. (a) Pale yellow tide (Diatom bloom) (b) brown tide (Trichodesmium bloom) (c) Red tide (Red Nocticula bloom) (d) Green tide (Green Nocticula bloom) (Source: Thangaraja et al., 2007).

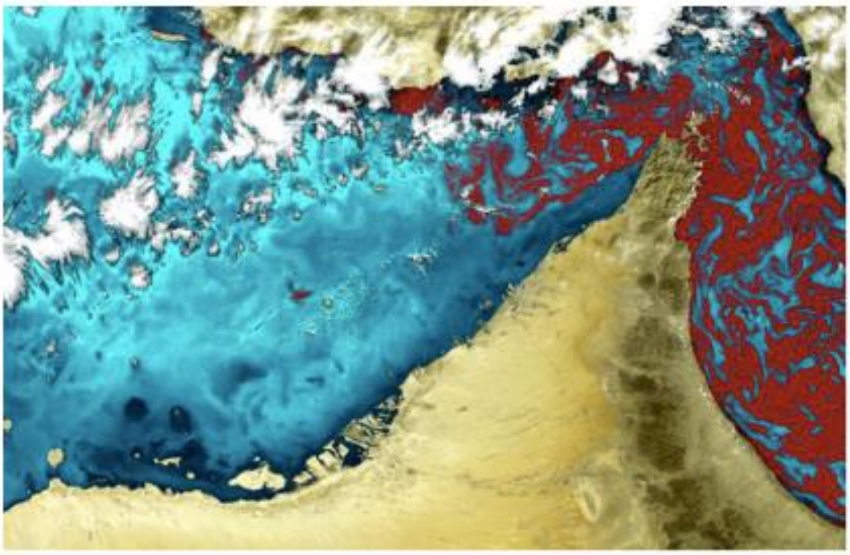

Figure 7: Large Red tide in the Oman Sea and Arabian Gulf. Composite image from the processing of a MERIS data acquired 22/11/2008. Data courtesy of EGU.

1.5.2 Occurrences and frequency:

Recent studies indicated an increase in the number, the frequency, the severity and the geographic distribution of HABs [26] [27] [28] [29] [30]. The Arabian Gulf , the Sea of Oman and the Arabian Sea have been regularly subject to HABs with outbreaks

recorded almost every year (Tables .1.2 and 3). The first HAB recorded in the history of Arabian Sea was in 1908 (Table 3) along the Indian coastline, where it extended from the Malabar Coast to Laccadive Islands [31] [32]. In the Arabian Gulf, Oman was the first country to encounter extensive HAB blooming activities in the 1970s (Table.2) [33].

Table 2: Frequency of HAB events recorded from 1996 to 2009 in the Arabian Gulf, and responsible species.

Arabian Gulf			
Country	**Year**	**Species**	**References**
UAE	2008-2009	*Cochlodinium polykrikoides, Dinophysis caudate, Dinophysis miles, Prorocentrum minimum, Pyrodinium bahamense, Ceratium furca, Pyrodinium bahamense*	Richlen et al. 2010 [34]
Iran	2008-2009	*Cochlodinium polykrikoides*	Saeedi et al. 2011 [35]
Kuwait	2001	*Gymnodinium impudicum, Pyrodinium bahamense.*	Glibert et al. (2002) [36]
Kuwait	1999	*Gymnodinium species*	(Heil et al. (2001) [37]
-	2000	-	Subba Rao et al., 2003 [38]
-	1999,	*karenia selliformis, Prorocentrum rhathymum*	Heil et al., 2001 [37], Al-Yamani et al., 2004) [39]
Iran	1999	*Karenia* species	Thangaraja et al. (2007) [33]
Kuwait	1997		Al-Yamani et al., 1997
UAE	1996	*Noctiluca scintillans*	Thangaraja et al. (2007) [33]

Kuwait	1988	-	Thangaraja et al. (2007) [33]
Qatar	1996	*Alexandrium* species, *Dinophysis* species, *Pseudo-nitzschia* species, *Gymnodinium breve*	Al-Ansi et al. (2002) [40]

Table 3: Frequency of HAB events recorded from 1988 to 2009 in the Sea of Oman and responsible species.

Sea of Oman			
Country	**Year**	**Species**	**References**
Oman	2008-2009	*Cochlodinium polykrikoides*,	
Oman	2005	*Noctiluca scintillans*, *Prorocentrum micans Trichodesmium erythraeum*	Al-Busaidi et al. (2008) [41]
Oman	2000	*Coscinodiscus* species	Al-Busaidi et al. (2008) [41]
Oman	1996	*Noctiluca scintillans*	Thangaraja et al. (2007) [33]
Oman	1995	*Prorocentrum arabianum*	Morton et al. (2002) [42]
Oman	1988	*Noctiluca scintillans*	Thangaraja et al. (2007) [33]
Oman	1978	*Gonyaulax* species , *Noctiluca* species	Thangaraja et al. (2007) [33]
Oman	1976	*Gonyaulax* species, *Noctiluca* species	Thangaraja et al. (2007) [33]

Table 4: Frequency of HAB events recorded from 1908 to 2005 in the Arabian Sea and responsible species.

Arabian Sea			
Country	**Year**	**Species**	**References**

India	2005	Trichodesmium erythraeum	Krishnan et al. (2007) [43]
India	2004	Noctiluca scintillans	Joseph et al. (2008) [44]
	2003–2004	Green Noctiluca	(Matondkar et al., 2004) [45]
India	2000	-	Thangaraja et al. (2007) [33]
-	1996	*Phaeocystis globosa, Nitzschia longissima, Novafabricia Bilobata, Navicula directa, Rhizosolenia hebetate, Rhizosolenia, stolterfothii, Rhizosolenia styliformis, Rhizosolenia alata, Chaetoceros didymus*	Madhupratap et al. (2000) [46]
Pakistan	1990	*Prorocentrum minimum*	Chaghtai and Saifullah (2001) [47]
India	1982	*Noctiluca scintillans, Trichodesmium* species	Padmakumar et al. (2012) [48]
Pakistan	1979	*Noctiluca scintillans*	Saifullah (1979) [49]
India	1979	*Fragilaria cylindrus*	D'Silva et al. (2012) [50]
India	1979	*Thalassiothrix longissima, Amphiprora species, Thalassiosira species*	D'Silva et al. (2012) [50]
India	1979	Cyanobacteria, dinoflagellates, diatoms	D'Silva et al. (2012) [50]
India	1935	-	D'Silva et al. (2012) [50]
India	1908	*Trichodesmium erythraeum, Noctiluca scintillans*	D'Silva et al. (2012) [50]

1.5.3 Effects

HABs are serious threats to marine ecosystem, tourism and other various effects. HABs have a great impact on many aspects for example the economic that can be seen in the seafood industries and businesses, tourism, and aquaculture operations. Human life can be disturbed as well as the social relationships and cultural practices tied to coastal resources for extended periods of time [51].

There are two different types of HABs-those that toxic which have an impact on wildlife death of human seafood poisonings and those which nontoxic that cause harm in the other ways [29].

Toxic HABs:

HABs can cause harm either due to their production of toxins [29]. Several toxic species of cyanobacteria, dinoflagellates and diatoms found in the marine environments, have led to several forms of human health impacts, especially by consumption of fish and shellfish. An example of Cyanobacteria bloom, *Trichodesmium thiebautii* species has been associated with human breathing problems .Dinoflagellates may cause human poisoning such as: Diarrhetic Shellfish Poisoning (DSP), Paralytic Shellfish Poisoning (PSP) and Neurotoxic Shellfish Poisoning (NSP). Diatoms may cause Amnesic Shellfish Poisoning (ASP). These toxins tend to accumulate up in the food chain becoming more concentrated at higher taxonomic levels. In this way, toxicity can cause severe health hazards even at a low abundance of toxin producers (this is particularly the case with Ciguatera), and even result in the meat of sharks and turtles becoming toxic. The primary vector for human poisoning is shellfish. HABs frequently result in large scale fish mortalities or shell fish poisoning which can adversely affect aquaculture, coastal tourism and fisheries. These can be caused by dinoflagellates (such as *Gymnodinium breve* and *G. mikimotoi*, which also

cause NSP, cyanobacteria (such as *Trichodesmium thiebautii*) and haptophytes (such as *Prymnesium parvum*, *Chrysochromulina polylepis* producing a toxin that increases the permeability of fish gills, resulting in osmoregulatory stress and death).

Nontoxic HABs:

Some HABs can decrease water quality and cause massive mortalities to natural populations of fish and marine mammals, including endangered and protected species, and can also damage coral reefs and shade submerged vegetation. The decrease of water quality by the changing of the water chemistry is related to dissolved oxygen, the reduction of light penetration, bacterial or fungal infection, smothering by mucus produced during blooms (Transparent Exoplymer Particles: TEPs), and the combination of these and other factors are possible causes of the mortality that may be associated with phytoplankton blooms. The depletion of oxygen occurs when phytoplankton release CO_2 and intake dissolved oxygen during the night of bloom periods. Some blooms achieve a high level of biomass. When this biomass decays as the bloom dies off, oxygen is consumed, leading to widespread mortalities of plants and animals in the affected area. These "high biomass" blooms are sometimes linked to excessive pollution inputs [52]. High density blooms of some diatoms, haptophytes and silicoflagellates (e.g. *Dictyocha speculum*), can clog fish gills causing suffocation.

For instance, the latest HABs (2008-2009) in the Arabian Gulf and the Oman Sea caused by *Cochlodinium polykrikoides* were the biggest threat to the marine environment.

Figure 8: Seventy tons of fish killed in Asmak fish farm, Quriyat. . (Source: Marine Fisheries Center, Ministry of Fisheries, Oman)

Consequently, these HABs killed one million tons of fish and benthic animals [53]. The fishing industry in the emirate of Fujairah located on the UAE's eastern shores has suffered from these HABs, and have affected the local waters, resulting in a large number of fish kills [54]. Figure 8 shows about 70 tons of fish killed in Asmak fish farm, Quriyat, Oman during these blooms. This type of mass mortality of marine organisms was recorded in the Sea of Oman twice, one at Al- Ghubrah in September 1988 and another at Barka in September 2000 [33]. In addition to that, these blooms caused a disturbance on coral community structures and, a variable mortality *of Acropora* specie in the Sea of Oman (from August 2008 until May 2009) [55]. Also , a high mortality rate was recorded of the shellfish *Solen dactylus* (razor clam) populations on the Golshahr coast of Bandar Abbas (in the northern coastal waters of the Arabian Gulf) [53]. Another example of HABs occurred in 1999, in Kuwait's waters and affected two HAB species namely, *karenia selliformis* and *Prorocentrum rhathymum* and caused a massive fish kill [56] [39].

1.5.4 Causes

Although the reasons for the increase of HABs outbreak are unclear, several have been suggested: (1) increased nutrient input to coastal oceans from human activities

[57] [58] [59] [24] (2) large-scale climactic changes (for example, global warming) [23] , (3) transport of toxigenic species in ship ballast water [60] , (4) increased use of coastal resources for shellfish harvesting and aquaculture [23] , and (5) increased surveillance by government health agencies and researchers [23].

The structure and abundance of the phytoplankton populations are mainly controlled by inorganic nutrients such as nitrogen, phosphorus, silica, and iron. Therefore, high nutrient concentration in water bodies is considered as the primary factor causing the HABs occurrence [57] [58].

1.5.5 Sources of nutrients

Several sources of nutrients can stimulate HABs, including mainly upwelling, land runoff, atmospheric deposition, and groundwater inflow, as well as agriculture and other fertilizer runoff. Yet another source is the growing aquaculture industry in many coastal areas [29]. Human activities such as dredging, land reclamation and land filling are worsening the situation by increasing nutrient levels of the water via dust and particulate matter [61].

Dust and atmospheric deposition:

The area around the Gulf is consider one of the main sources of aeolian dust in the world [62].The strong wind events in this region are often associated with dust storms. Dust particles swept over the sea surface agglomerate into larger and heavier particles with high settling velocities [63]. Dust deposition enriches sea waters with micronutrients (e.g., iron), stimulating phytoplankton growth in iron-limited zones [64] [65] [66] [67] [68] and it is an essential factor regulating phytoplankton growth in the Gulf [69]. Nezlin et al. (2010) showed that the atmospheric deposition is an important factor regulating phytoplankton growth in the Arabian Gulf. In fact, dust

storms constitute a major ecological force by strongly influencing pelagic production in waters of the arid zone and tested whether dust storms enhance phytoplankton growth in Kuwait coastal waters [70] because a greater input of iron (Fe) occurs with inputs of dust [71].

Upwelling:

Upwelling is an oceanographic phenomenon and because of winter storm events it rises seasonally in temperate environments. This phenomenon involves wind-driven motion of dense, cooler, and usually nutrient-rich water towards the ocean surface, replacing the warmer, usually nutrient-depleted surface water. The reproduction of primary producers such as phytoplankton is catalyzed by the nutrient-rich upwelled water. Due to the biomass of phytoplankton and presence of cool water in these regions, and upwelling zones can be identified by cool sea surface temperatures (SST) and a high concentrations of chlorophyll-a.

The deep part of the Gulf is characterized by pronounced hyaline stratification [72] [73] [74]. In contrast, the water column in the shallow (<10–15 m) northern, western and southern Gulf is well mixed, as a result of wind stress and tidal turbulence [75]. Persistent northwesterly winds produce southeastward coastal currents and has caused upwelling along the northeastern (Iranian) coast and down welling along the southwestern (Saudi) coast [73]. The circulation in the Sea of Oman is well known by a clockwise gyre in the west and a counter-clockwise gyre in the east, creating a region of upwelling along the Iranian coast at the interface between the two [73].

Rivers discharge:

The Shatt Al-Arab estuary is the only northern source of freshwater inflow into the Gulf. This is considered a source of nutrients to the Arabian Gulf [76]. The rivers Tigris and Euphrates each annually discharge 45.3 x 10^6 m^3 of water, and carry 57.6 x 10^6 and 4.8 x 10^6 t sediment, respectively [73].

Ballast water from tankers:

The Regional Organization for the Protection of the Marine Environment (ROPME) Sea Area is the largest recipient of ships' ballast water with annually more than 45,000 vessels visit this area and discharge a large amount of ballast water [77]. This ballast water has an anthropogenic cause, like sewage, which has been considered as a significant factor behind the increasing occurrence of HABs [60].Ballast water from shipping traffic can transfer a range of species of microalgae, including toxic species that may form harmful algae blooms [78]. Phytoplankton transport by means of ships ballast water has been regarded of paramount importance to explain the worldwide distribution of some phytoplankton species [79] [80], including bentho-planktonic forms of toxic dinoflagellates [81]. For instance, the introductions of *Cochlodinium polykrikoides* species, responsible for the catastrophic HABs in 2008-2009 in the Arabian Gulf region, was through ballast water discharge [34].

1.5.6 Detection of HABs: advantages of satellite observations

Different approaches have been used for algal bloom detection. Ship observations and buoy stations are conventional methods but consuming. Furthermore, they are temporal-spatial coverage limited. For example, a ship survey station may cover an area within 1m in the vicinity of the ship. On the other hand, the circumstances of

algal blooms could be affected by ship based sampling, which can have effects on the accuracy of sampling results. Therefore, an alternative is desired.

Satellite measurements have shown to be more effective in applications of algal bloom detection and tracking, thanks to their high spatial and temporal coverage over large scales. They can complement local *in situ* measurements. Furthermore, satellite measurements can cover larger and remote areas. Oceanographic researches have entered a new era since the launch of the first ocean color satellite sensor, namely the Coastal Zone Color Scanner (CZCS) onboard Nimbus 7 in 1978. The Sea-viewing Wide Field-of-view Sensor (SeaWiFS, 1997-2010) with a spatial resolution of 1000 m at nadir collected 13-year of daily global imagery and they are made freely available to the scientific community by NASA. Access to satellite imagery from several other sensors is also open, such as MODIS onboard Terra (1999-present) and Aqua (2002-present) satellites, MEdium Resolution Imaging Spectrometer (MERIS, 2002-2012), and Visible Infrared Imaging Radiometer Suite (VIIRS, 2011-present). The new era of open-access satellite data will augment the use of satellite imagery for bloom detection and monitoring.

In contrast with the numerous applications of satellite imagery for algal bloom observation, satellite based detections of algal bloom in the Arabian Gulf and its adjacent area is still in its initial period. Moradi and Kabiri (2012) used Moderate Resolution Imaging Spectroradiometer (MODIS) fluorescence data to detect the 2008 red tide with more focus on the Strait of Hormuz and the eastern region of the Arabian Gulf. Hamzei et al. (2012) have also investigated the 2008 red tide event using MODIS images and suggested that upwelling and sewage were the key nutrient sources that trigged the bloom in the Arabian Gulf and the Sea of Oman. Zhao and Ghedira (2014) used multi-sensor data to track the harmful algal bloom in

the Gulf region and their analysis suggested that the bloom was probably caused by upwelling. A regional algorithm was also developed by Zhao et al. (2015) to qualitatively separate algal blooms dominated by different phytoplankton blooms.

Different approaches based on satellite measurements have been proposed to indicate the occurrence of algal bloom, such as chlorophyll-a concentration, and fluorescence line height (FLH). However, their accuracy is still problematic. The operational chlorophyll-a algorithm is based on the blue to green ratio of radiance. It works well for case I waters where other optically active components co-vary with phytoplankton. As with case II waters, the empirical band ratio algorithm fails due to the effects of water substituents whose optical properties vary independent upon phytoplankton. Although the FLH approach was successfully used to detect and trace algal blooms, it is sensitive to suspended sediments and benthic vegetation. Therefore, a regional effective tool needs to be developed.

CHAPTER 2

HABs and Desalination

2.1 Definition

Desalination is the process of removing salt (sodium chloride) and other minerals from water to make it suitable for human consumption (potable) or for other uses e.g. irrigation, industrial (non-potable) since many countries suffer from limited supplies of fresh water. The worldwide feed-water percentage used in desalination accounts 67%, 19%, 8% and 6%, respectively for seawater, brackish water river water, and wastewater desalination production [82]. The most prolific users of desalinated water are in the Arab region, namely, Saudi Arabia, Kuwait, United Arab Emirates, Qatar, Oman, and Bahrain [83].

Figure 9 shows the global desalination capacity in m^3/d and percentage including all source water types: seawater, brackish and waste waters (IDA, 2008). This figure from the 20th IDA Worldwide Desalting Plant Inventory indicate that about 28 million cubic meters per day (Mm^3/d) are presently produced from seawater sources [84]. Three quarters of this water is produced in three sea areas: the Arabian Gulf, the Red Sea, and the Mediterranean Sea [85].

2.2 Desalination in the Arabian Gulf:

The "hot spot" of intense desalination activity has always been the Arabian Gulf [86]. In fact, almost 60% of the freshwater supplies rely on desalination plants for countries around the Arabian Gulf [87].

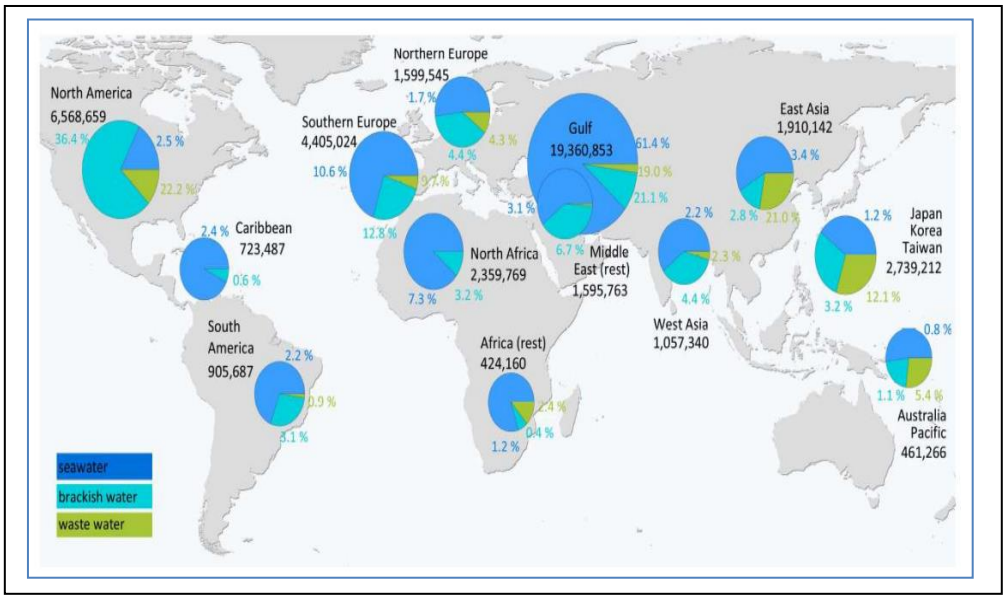

Figure 9: Global desalination capacity in m3/d and % including all source water types (seawater, brackish and wastewaters) (IDA, 2008).

The installed capacity in the Gulf is 19,360,853 m^3/d as shown in figure 9. The figure, next to the pie diagram, gives the contribution to the global production, i.e., the seawater desalination capacity in Gulf represent 61.4 % of the global seawater desalination capacity. The brackish water capacity - though it is less than half the seawater desalination capacity - represents 21.1% of the global brackish, and the wastewater 19 % of water desalination capacity. Seawater desalination accounts for most of the production in the Gulf, brackish water for about 1/5 of the production and wastewater desalination plays a relatively minor role (pie diagram) [84].

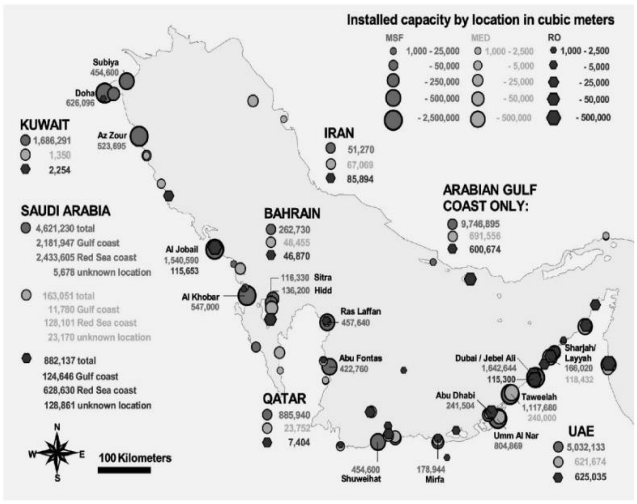

Figure 10: Seawater desalination capacities in the Arabian Gulf (Source: Dawoud and Al Mulla., 2012).

The United Arab Emirates is the major producer of fresh water from desalination 35% in the Gulf followed by Saudi Arabia 34%. The other countries like Kuwait is 14%, Qatar (8%), Bahrain (5%) and Oman (4%) [88].

2.3 Desalination technologies

Desalination technologies are divided to two parts **thermal** or **membrane**. The main desalination processes are summarized in Table 5. The two technologies thermal and membrane desalination has varied advantages and disadvantages depend on specific parameter. A combination of these two technologies also can be used in water purification plants.

Table 5: Desalination technologies and process

Thermal Technology	Membrane Technology
Single-Stage Distillation (SSD)	Reverse Osmosis (RO)
Multi-Stage Flash Distillation (MSF)	Electrodialysis (ED)
Multi-Effect Distillation (MED)	Electrodialysis reversal (EDR)
Vapor Compression Distillation (VCD)	

2.3.1 Thermal technology:

In thermal technology, as the name implies, saline water is heated to form steam that cools and condenses to form purified water (distillate) while the Inorganic compounds and large non-volatile organic molecules do not evaporate with the water and are left behind. Due to the high cost thermal technologies have not been used for brackish water desalination. However, they have been used for seawater desalination and can be sub-divided into four groups: Thermal technologies divide to Single-Stage Distillation (SSD), Multi-Stage Flash Distillation (MSF), Multi-Effect Distillation (MED) and Vapor Compression Distillation (VCD).

(i) Single-Stage Distillation (SSD):

In SSD, the saline water is heated in the steam heat exchanger. The steam passing the tubes will condense again in the boiler, while the saline water outside the tubes will evaporate to the condenser tank and be cooled down by the cooled water pipes in such a way vapor will turn to pure liquid. The vapor pressure of the saline is reduced, in order to decrease the boiling temperature because the boiling temperature should not

exceed the temperature of the condensation steam. This method is applicable for marine application and big laboratories.

(ii) Multi-Effect Distillation (MED)

For the heat recovery principle, MED was developed, where the vapor from each evaporator will serve as heating steam for the next evaporator while at the same time, the boiling saline in the evaporator will serve as condensing medium for the vapor. Thus, the greater the number of evaporators, the less heating steam will be needed.

(i) Multi-Stage Flash Distillation (MSF)

Regarding MSF, multi stages act as an evaporator to increase efficiency, but on the other hand, they also increase the cost and the scale formation.

(ii) Vapor Compression Distillation (VCD)

VCD uses a mechanical source, which is a vapor compressor for the required heating steam needed to boil saline water. To increase the performance of the mechanical vapor compression pilot plant, the compressor speed should be increased, and the concentration of the brine should be decreased. So, the difference between the VCD and the other two types MED and MSF is the heating source [89].

2.3.2 Membrane procedures:

Membrane Technology uses a membrane to separate the salt from water. Membrane Technologies can be divided into categories - Reverse Osmosis (RO), Electrodialysis (ED) and Electrodialysis reversal (EDR).

(i) Reverse Osmosis (RO),

In RO, the water will diffuse through a semi-permeable membrane into a solution to achieve equilibrium. This occurs until sufficient hydrostatic pressure develops to offset the osmotic pressure. Seawater is divided into fresh water free of particulates and dissolved impurities, and the brine enriched water with suspended and dissolved solids.

(ii) **Electrodialysis (ED)**

ED depends upon a selective permeable membrane charged with an electrical potential to separate solutes of different ionic or molecular size in a solution by a driving force. This force is the driving force for dialysis and the difference in the solute concentration across the membrane.

(iii) **Electrodialysis reversal (EDR) :**

EDR works with the same concept as electrodialysis, except that the polarity of the DC power is reversed to two to four times per hour reversal valves, which prevents the formation of scale on the membrane[90].

2.4 **Desalination discharge**:

The overall procedure of seawater desalination is similar in most cases. The procedure is the separation of the pre-treated water (saline water) into two parts:

- **Treated water :**a highly pure product with a low concentration of salt (drinking water)
- **Wastewater:** refers to brine or ‘concentrate’ with a much higher concentration than the original feed water. This by-product of the desalination process (brine) is concentrated salt water containing a mixture of chemicals used during plant

operation to be disposed of or recycled. At present, it is mostly discharged into the sea or diluted and sprayed into an open space.

Several types of chemicals (Table 6) are used in the desalination process for pre- and post-treatment operations and cleaning at variable concentrations. Often these chemicals are discharged to the sea water as part of waste brine [91] [92] [93].

Table 6: Types of chemicals used in the desalination process for pre- and post-treatment operations [86]

Chemicals	Use
Sodium hypochlorite (NaOCl)	Used for chlorination to prevent bacterial growth in the desalination facility
Ferric chloride ($FeCl_3$) or aluminum chloride ($AlCl_3$)	Used as flocculants for the removal of suspended matter from the water
Sodium hexametaphosphate $(NaPO_3)_6$	Used to prevent scale formation on the pipes and on the membranes
Sulfuric acid (H_2SO_4) or hydrochloric acid (HCl)	Used to adjust the pH of the seawater.
Heavy Metals (Copper-nickel alloys)	Used as heat exchanger materials
Chlorine	Added to the intake water to reduce biofouling
Sodium perborate and formaldehyde	Biocides (to kill bacteria)

The brine discharge has negative affect on the marine environment as it can change the water temperature, salinity as well as the alkalinity[73]. In most cases, the high temperature doubled the salinity and total alkalinity of the discharge brine than the normal conditions. As an example, the salinity of the brine that produced from RO plants has a salinity up to twice that of sea water [76]. This lead to an increase in the overall salinity and in the case of undiluted, the brine will stratify below the less dense seawater [94] [95].

2.5 **The impacts of desalination plants discharge on the marine environment**:

Many environmental impacts can be caused by desalination plant as any other industrial activity (liquid and solid waste) to the surrounding area and to the atmosphere (gas emission). Main causes are linked with the brine discharge as it has a massive impact on the environmental aspect [96]. Marine life has a high influent from desalination plant. Chemical and physical characteristic of the brine has a huge rule in these impacts. At the moment, there are no specific assizes to control the physical parameters and chemical concentrations of brine effluents resulting from the desalination processes [81]. The impacts associated with brine discharges into seawaters are related to:

- Effects on water quality: by the increasing of salinity, temperature and alkalinity [86], and by the potential chemical pollution, and by the turbidity (because of the presence of hyper saline effluent) [81].

- Impacts on algal population growth, seagrasses and plankton: macroalgae and seagrass are sensitive to potential impacts from RO waste brine [97]. The population levels of the algae depend primarily on water quality (e.g., turbidity, salinity, temperature, dissolved oxygen content, nutrient concentrations, etc.) and changing water quality can trigger algal population growth. The turbidity affects seagrasses by reducing the percentage of light filtered through the water column that reaches the seabed, thus affecting seagrass photosynthesis [98]. The impact on plankton is by causing a drop in osmotic pressure and hence causing negative effects in primary production [81].

- Impacts on fish fauna: extinction of the fish larvae and younger individuals of these community in turbid areas and emissions associated with the brine and cleaning water discharges [99].

- Effects on coral reefs, which are very sensitive to changes in environmental conditions (chemical pollution, hydrodynamic alterations, temperature, salinity, etc.), and thus, brine disposal may have significant negative effects [81]. Elevated concentrations of trace metals such as copper, lead, zinc, calcium and nickel can also reduce the fertilization success of Scleractinian corals [100].

- Effects on primary productivity (HABs): the addition of nitrogen and iron during the RO process has potential to affect primary productivity, as they are potentially limiting elements in marine systems [101]. In addition to that, the increase of temperature in the water bodies classified the desalination plant discharge among the factors behind the increasing occurrence of HABs [24].

However, it is needed to set a probable solution for the disposal and brine due to their unfavorable environmental impacts[102]. Extensive knowledge of the effluent properties and the receiving environments is required in order to estimate the potential impacts of desalination plants on the marine environment.

2.6 **The effects of the marine environment on desalination plant**:

The effects of the marine environment on the plant are recognized primarily as biofouling of the intake structures, pumps and various plant structures. The biofouling or biological fouling is the accumulation of microorganisms (e.g. bacteria and phytoplankton) and macroorganisms (caused by a variety of invertebrate organisms and marine algae). The presence of phytoplankton can cause a reduction in

desalination plants production by up to 40% [24]. Microfouling induced corrosion and macrofouling induced failures have been reported in the literature [103]. The emerging threat to the desalination industry is from HABs. This threat from HABs to desalination plants is not new, but is growing in scale and significance, due to the expansion of both HABs and desalination plants globally. High biomass HABs can restrict flow in desalination plants by clogging filters and increasing membrane fouling rates in microfiltration systems that are frequently incorporated, or considered, in today's desalination facilities [104] [105] [106]. These fouling of surfaces due to dissolved organic materials, can also compromise the integrity of reverse osmosis (RO) membranes.

The last HABs outbreak, which lasted nearly eight months in the Gulf-Arabian Sea region in 2008/2009, is a clear example of the risk posed by these phenomena. The bloom of the dinoflagellate *Cochlodinium* forced the closures of at least five seawater desalination plants in the UAE due to clogging of intake filters (Fig11),

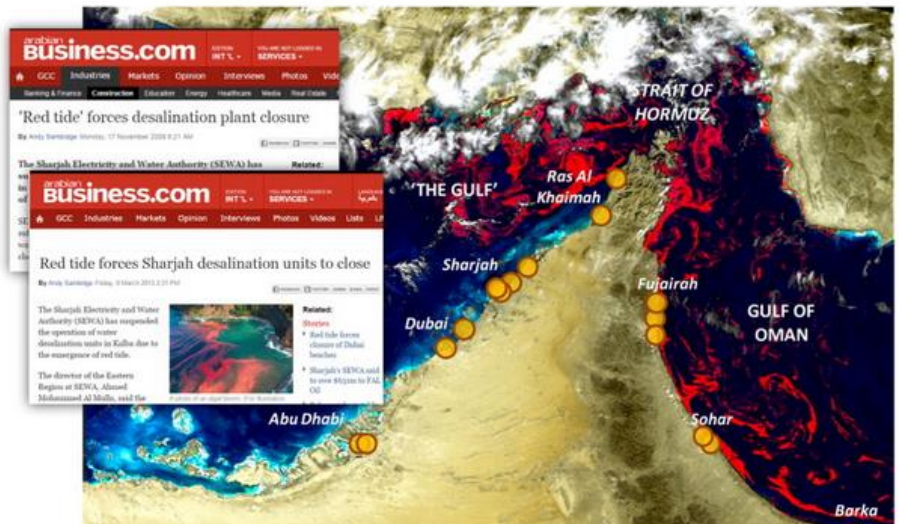

Figure 11: A massive "red tide" algal bloom in the Gulf of Oman spreading to the Gulf from the satellite image obtained by the European Space Agency MERIS (source Villacorte et al., 2015)

concerns that the bloom would irreversibly foul RO membranes, or other operational problems caused by the dense blooms [107] [108].

Toxic HABs have been recently recognized as a threat to desalination plants where the chemical structures of toxins can persist in desalinated water and cause threats to human health [109].

Because of the increasing trend in HAB occurrence throughout the region, it is very important to protect membrane-based desalination plants during an algal bloom. Early detection will serve as a good indicator for desalination plants to take the necessary steps to prevent severe fouling and provides the necessary time for preventative measures. Such detection will have information on certain parameters such as turbidity, silt density index (SDI), dissolved oxygen, and bulk fluorescence [110]. However, this measurement is not enough to detect the growth of algal blooms. Protecting membrane-based desalination plants can be done by developing methods and techniques to better understanding and characterizing the membrane fouling potential of algae and algal organic matter (AOM) as the studies have been conducted over limited spatial and temporal scales. In any algal blooms event, it is essential to emphasis on important processes such as the intakes because of the subsurface accumulations of algae, toxin removal during treatment and removing algal biomass during pretreatment [111]. The challenge that desalination plants face over the world is the diversity in species, bloom types, and impacts with tens of thousands of species of algae in the oceans [112].

Granular media filters (GMF) for the pretreatment process proved that it is possible to reduce the penetration of algae, but at the same time cannot stand in the face of (AOM), and in particular, transparent exopolymer particles (TEPs), as it can still pass through the pre-treatment systems and lead to a fouling in the downstream RO system

[113]. As a solution to this drawback of the GM, it was proposed to add a dose of coagulant in front of the GMF. This however, may cause another problem by increasing the rate of clogging in the filter. This happens because of the high biomass accompanied by high filtration rate (5-10 m/h) in the granular filters[114]. One possible solution is to install dissolved air flotation (DAF) in front of the GMF, as it will reduce clogging problems by increasing the coagulant dose and improving effluent quality. Another solution is to replace GMF with ultrafiltration (UF) or microfiltration (MF) membrane systems. The only drawback in UF and MF, is the rate of fouling during algal bloom periods. This can be overcome by adding a DAF system prior UF/MF system[115].

CHAPTER 3

Methodology

3.1 Red tide index (RI)

In the literature, the monitoring of algal blooms has been mainly focused on the quantitative determination of chlorophyll-a concentration and fluorescence line height (FLH). However, these approaches have limitations. Satellite derived chlorophyll-a concentration are problematic for regional use, especially in coastal waters, as the operational algorithm was designed for Case I waters. Although FLH has been successfully used for bloom detection, it can be affected by suspended sediments and variations in environmental conditions (such as light and nutrient). Therefore, alternatives are needed.

Ahn and Shanmugam (2006) developed a red tide index (RI) for bloom detection in Korean South Sea, East China Sea, Yellow Sea, and Bohai Sea, using Sea-viewing Wide Field-of-view Sensor (SeaWiFS) data. Shanmugam (2011) showed that RI is maximally sensitive to variability of algal bloom and minimally to other optically active constituents besides phytoplankton, i.e., suspended sediment, colored dissolved organic matter, and detritus. However, to the best of our knowledge, a red tide index for monitoring algal blooms in the entire Arabian Gulf has never been reported before. This research project proposes to monitor red tides in the Arabian Gulf using a qualitative index, namely, RI, as an alternative to quantitative methods. We expect

that the qualitative index should be more straightforward to determine especially over long periods. The research will also pursue the comparison of the qualitative index to *in situ* observations of chlorophyll a concentration and other water quality parameters. Ahn and Shanmugam (2006) used SeaWiFS data for bloom detection. However, the SeaWiFS sensor retired in 2010. For the purpose of continuity, Moderate Resolution Imaging Spectroradiometer (MODIS) data are used instead. MODIS sensors are onboard two satellites, Terra (2000-present) and Aqua (2002-present), which overpasses local areas in the morning and afternoon, respectively. Since MODIS/Terra data suffer from the striping issue, only Aqua data were considered in this project. Global changes can be traced accurately enough by MODIS, which in return can assist researchers to predict and improve the overall understanding of the environment.

3.2 In situ data

Chlorophyll-a pigment is present in most plants as well as in algae that is why it is a convenient indicator of algal biomass. During in situ sampling trips, water samples were collected from 36 stations (as shown in figure 12) to determine chlorophyll a concentration. Chlorophyll a concentrations were recorded after series of laboratory procedures on the water samples, which include filtration and spectrophotometric detection by a spectrophotometer (Perkin Elmer Lambda 25), as shown in figure 13. Chlorophyll-containing phytoplankton in a measured volume of sample water, are concentrated by filtering at low vacuum through a Whatmann GF/C filters (45 µm in pore size, and 47 mm in diameter). The filters were folded and stored in the freezer at -20ºC until extraction.

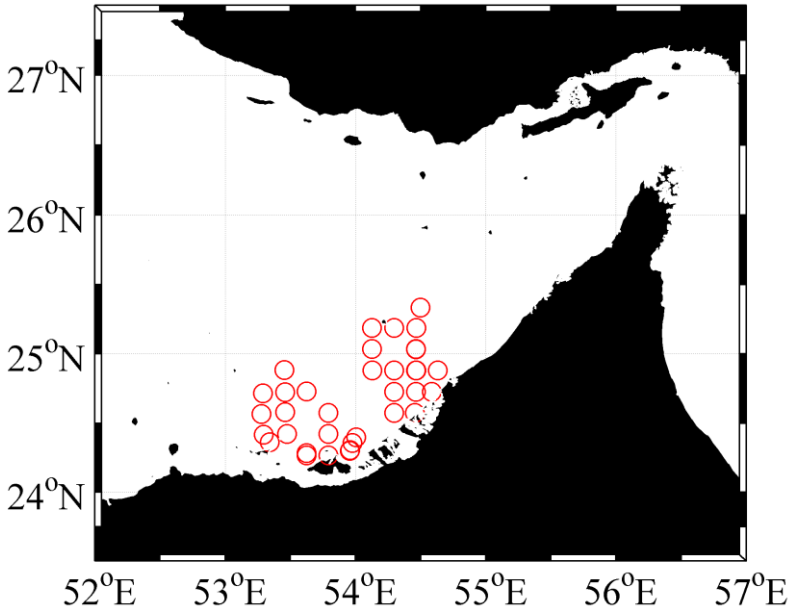

Figure 12 :. In situ stations where water samples were collected during our field surveys along the west coast of the UAE.

The pigments were extracted from the phytoplankton in 90% acetone (5mL) in centrifuge tubes in cold and processed with freezing and sonication to ensure thorough extraction of the chlorophyll. The samples were disrupted by sonication in darkness in an ice bath and homogenized at 20000 rpm for 15s, until the filter was completely disrupted and allowed to extract at -20ºC for 24 hours.

The pigment extracts were centrifuged at 5,000 rpm during 10 min (centurion scientific K3 Series). To reduce the turbidity interference, the supernatant was transferred an inert centrifuge tubes and re-centrifuged. The supernatant solutions were harvested and used to determine their optical densities in 664 nm and 750 nm for turbidity correction. The Chl-*a* concentrations were determined by the spectrophotometry analysis using a Perkin Elmer spectrophotometer (Lambda 25).

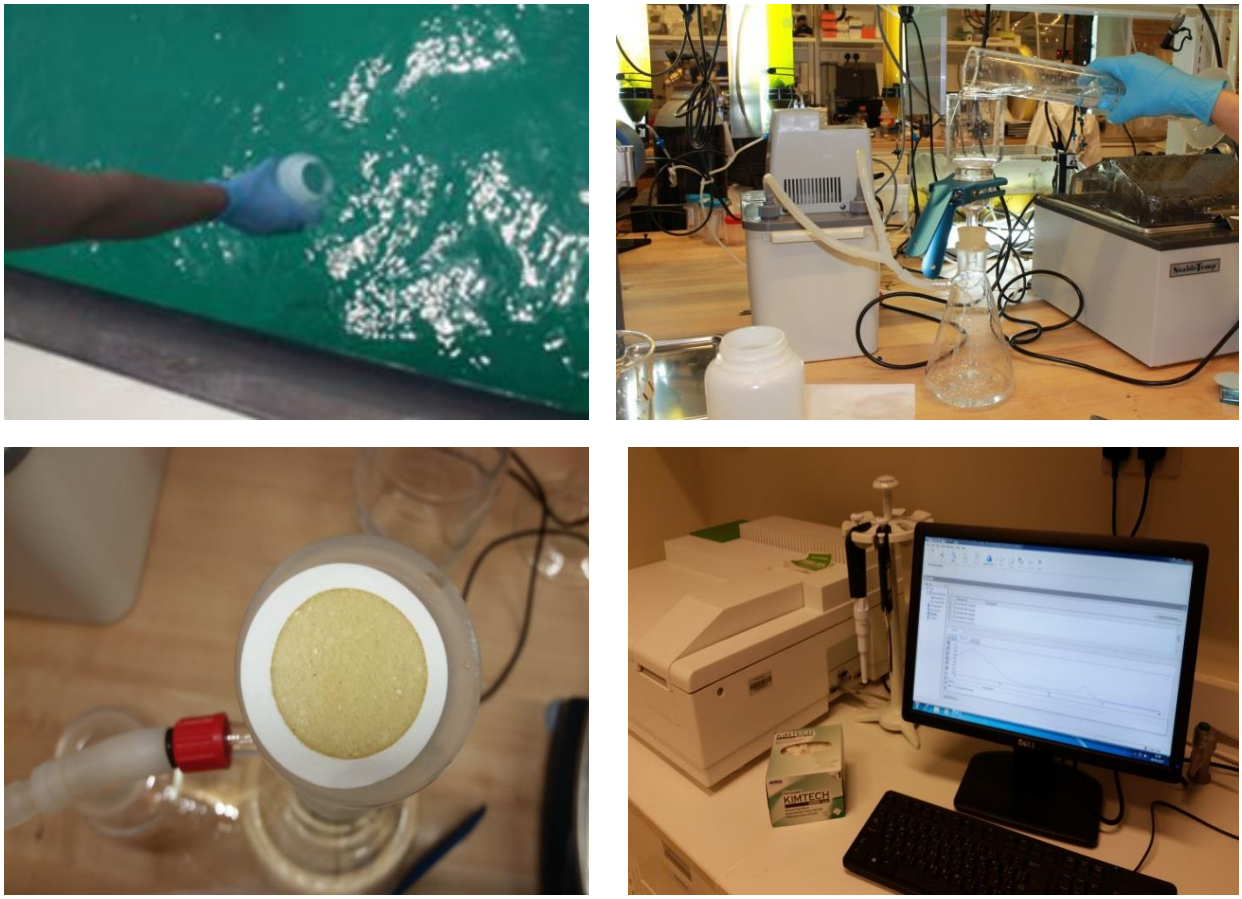

Figure 13: Examples of pictures for water sampling, filtration, filter pads of water samples, and the instrument to determine chlorophyll-a concentration, i.e. Perkin Elmer spectrophotometer.

The Chl-*a* concentration was calculated using Ritchie (2006), empirical correlation to evaluate the concentration of *chl-a*, which uses the followed formula:

Richie (2006)

$$\mu g_{\text{chlorophyll}}/_{mL_{medium}} = 11.4062\, A_{\mathbf{664}}\, {}^{v}/_{lv}$$

$$\mu g_{\text{chlorophyll}}/_{mL_{medium}} = 11.4062\, A_{\mathbf{664}}\, {}^{v}/_{lv}$$

Where

A_{664}: The absorbance at 664 nm, after removing the sample absorbance at 750nm, against a blank of the used solvent.

v : The volume of solvent used (mL)

l: The spectrophotometric cell length (cm) and

V: The sample volume used (mL).

Remote sensing reflectance (R_{rs}) data were collected following the NASA ocean optics protocol. It is briefly described there. A hyperspectral radiometer (Ocean Optics USB 2000+) with a spectral resolution of 1 nm was used. The spectra range from 350 nm to 900 nm. The field-of-view angle is 10°. The radiance signals reflected from the water surface (L_{water}), sky (L_{sky}), and a gray plaque (L_p) were measured, which were then used to calculate R_{rs}. The equations are expressed below:

$$R_{rs} = \frac{L_w}{E_s}$$

$$L_w = (L_{water} - \rho L_{sky}) * F_L$$

$$E_s = \frac{\pi L_p}{R_p} * F_L$$

Where ρ is the Fresnel reflectance of the air-sea interface and an empirical constant of 0.028 was used. F_L is the sensor response signal when the gray plaque was viewed at a fixed angle of 90°. R_p is the bi-directional reflectance function (BRDF) of the gray plaque. Both F_L and R_p data were provided by the manufacturers.

3.3 Deployment of a regional red tide index:

With respect to satellite imagery, MODIS/Aqua data were used to calculate RI in this study. The MODIS instrument has a viewing swath width of 23,330 km. It has a revisit frequency of one day. It measures 36 spectral bands between 0.405 and 14.385 μm with different spatial resolutions: 250 m, 500 m and 1000 m. 9 visible bands, which are centered at 412, 443, 488, 531, 547, 667, 678, 748, and 869 nm, respectively, with a spatial resolution of 1000 m were designed for ocean color

studies. A quick review of the literature showed that the bands used for the design of RI were located in the blue-green region. Although our field measured L_w data covered the spectral range between 350 and 900 nm, only those bands corresponding to MODIS ocean color bands were considered in order to expand the designed model to satellite applications. To identify the most reliable model to quantify RI, four models were compared, which were formulated as follows:

$$RI_1 = \frac{L_w\_488/L_w\_547 - L_w\_443}{L_w\_488/L_w\_547 + L_w\_443} \quad (1)$$

$$RI_2 = \frac{L_w\_531/L_w\_547 - L_w\_443}{L_w\_531/L_w\_547 + L_w\_443} \quad (2)$$

$$RI_3 = 10^{\frac{L_w\_488/L_w\_547 - L_w\_443}{L_w\_488/L_w\_547 + L_w\_443}} \quad (3)$$

$$RI_4 = 10^{\frac{L_w\_531/L_w\_547 - L_w\_443}{L_w\_531/L_w\_547 + L_w\_443}} \quad (4)$$

RI_1 and RI_3 used 488, 547 and 443 nm while RI_2 and RI_4 used 531, 547, and 443 nm. The 412 waveband was not considered since this band is subject to atmospheric correction failure when algal bloom conditions were encountered.

3.4 Satellite data processing

MODIS/Aqua L0 data were obtained from NASA ocean color data archive. SeaWiFS Data Analysis System (SeaDAS) software package developed by the NASA Ocean Biology Processing Group (OBPG) used to process satellite imagery. The default near infrared (NIR) atmospheric correction scheme was carried out, which assumes that the

radiance in the NIR region is negligible. The default blue-green band ratio algorithm for chlorophyll-a concentration was implemented. Output products included normalized L_w (nL_w) at 443, 488, 531, and 547 nm, sea surface temperature (SST), level-2 flags, and chlorophyll-a concentration. Enhanced Red-Green-Blue (ERGB) images were composited with nL_w at 547 (R), 488 (G), and 443 (B) nm. The 547 nm was used as the red band instead of 667 nm for the ERGB images because nL_w at 667 nm is low and does not provide adequate information, especially for case I waters. Data form 2002 to 2014 was processed and 2406 scenes were obtained. The whole gulf region bounded by 23.2°-30.7° N and 47.3°-56.5° E was investigated. The spatial resolution of the processed scenes was 1000 m.

CHAPTER 4

Result and Discussion

4.1 **Results from in situ measurements**

The *in situ* measured R_{rs} spectra between 400 and 750 nm are shown in figure 14. The spectra show the characteristics of typical case II waters. The spectra indicate peaks between 490 and 560 nm, which are determined by the absorption and backscattering properties of optically active components, including phytoplankton, colored dissolved organic matter (CDOM), non-algal particulate, and pure water. The spectral peak around 650 nm appears due to the prominent absorption by chlorophyll-a and phycocyanin on both sides of the peak and the phycocyanin fluorescence emission at 640 nm [116]. The peak around 685 nm is due to the emission of chlorophyll-a fluorescence stimulated by sunlight. The peak height of chlorophyll-a fluorescence has been used as a proxy of chlorophyll-a concentration.

Chlorophyll-a concentrations of 36 stations from our field surveys are used in this study. The histogram of *in situ* measured chlorophyll-a concentration is presented in figure 15a. Chlorophyll-a was ranged between 0.08 and 1.88 mg m^{-3}. Ten and eight data points were located in the range of 0.2-0.4 and 0.4-0.6 mg m^{-3}, respectively. The highest chlorophyll-a was collected in fall while the lowest chlorophyll-a was found in summer. This is consistent with previous findings by Nezlin et al. (2010). Regarding the spatial distribution, the chlorophyll-a map is displayed in figure 15b. It indicates that chlorophyll-a increased along the tracks from onshore to offshore. This

is totally different from cases for other regions in the world. This can be very likely related to the small, even ignorable, terrestrial runoff in the region, which can bring nutrient-rich waters to the coastal zone and support the growth of phytoplankton.

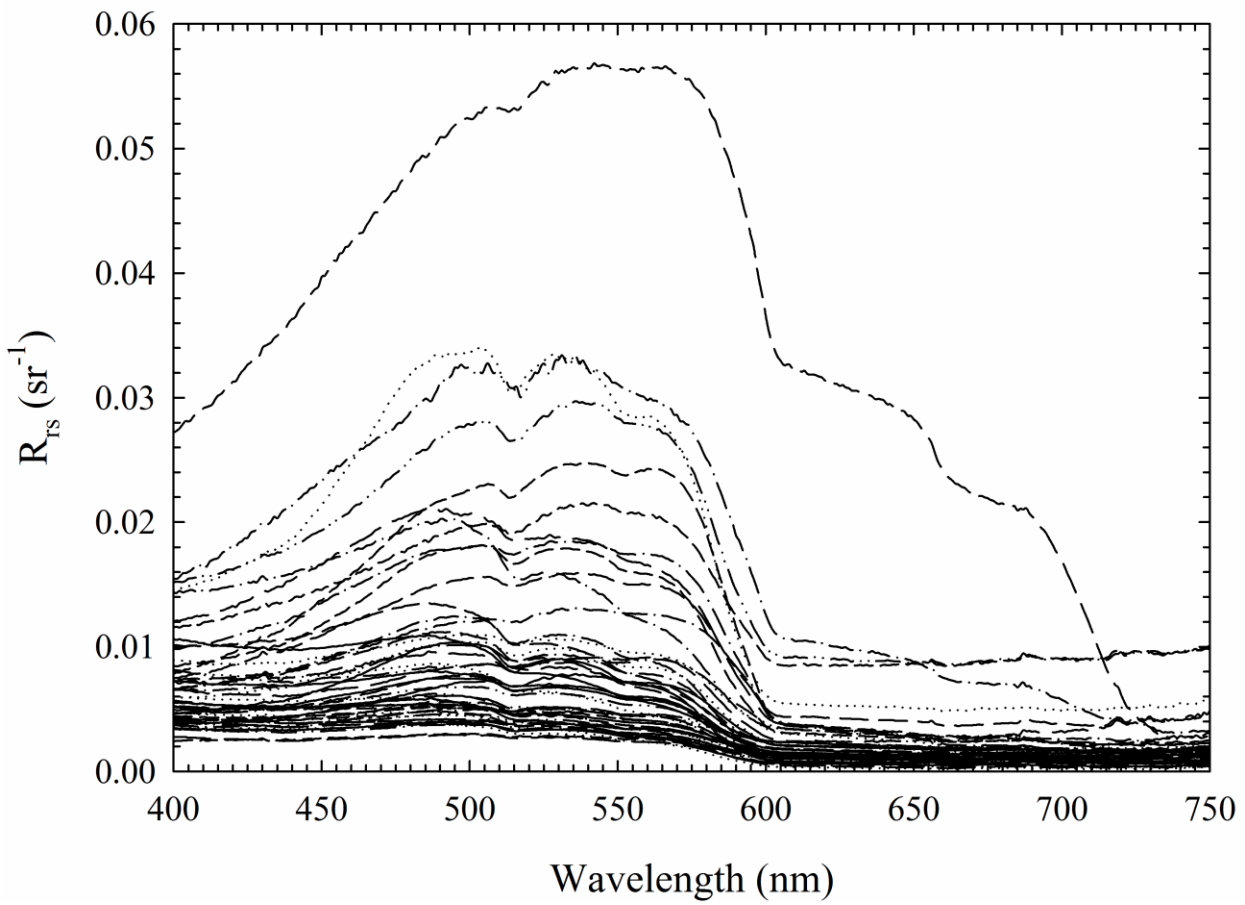

Figure 14: Remote sensing reflectance (Rrs) spectra between 400 and 750 nm for those stations shown in figure 12 measured during our field campaigns.

4.2 **Validation of the proposed red tide index**:

36 data points were randomly divided into two parts, nominally 19 and 17 for algorithm development and validation, respectively. In order to identify which model developed performs the best, the four models are plotted against chlorophyll-a concentration, as shown in figure 16. The determination coefficient for RI_1 vs chlorophyll-a based on a quadratic method is 0.69, 0.67 for RI_2 vs chlorophyll-a, 0.68

for RI_3 vs chlorophyll-a, and 0.67 for RI_4 vs chlorophyll-a, respectively. The equations are listed below:

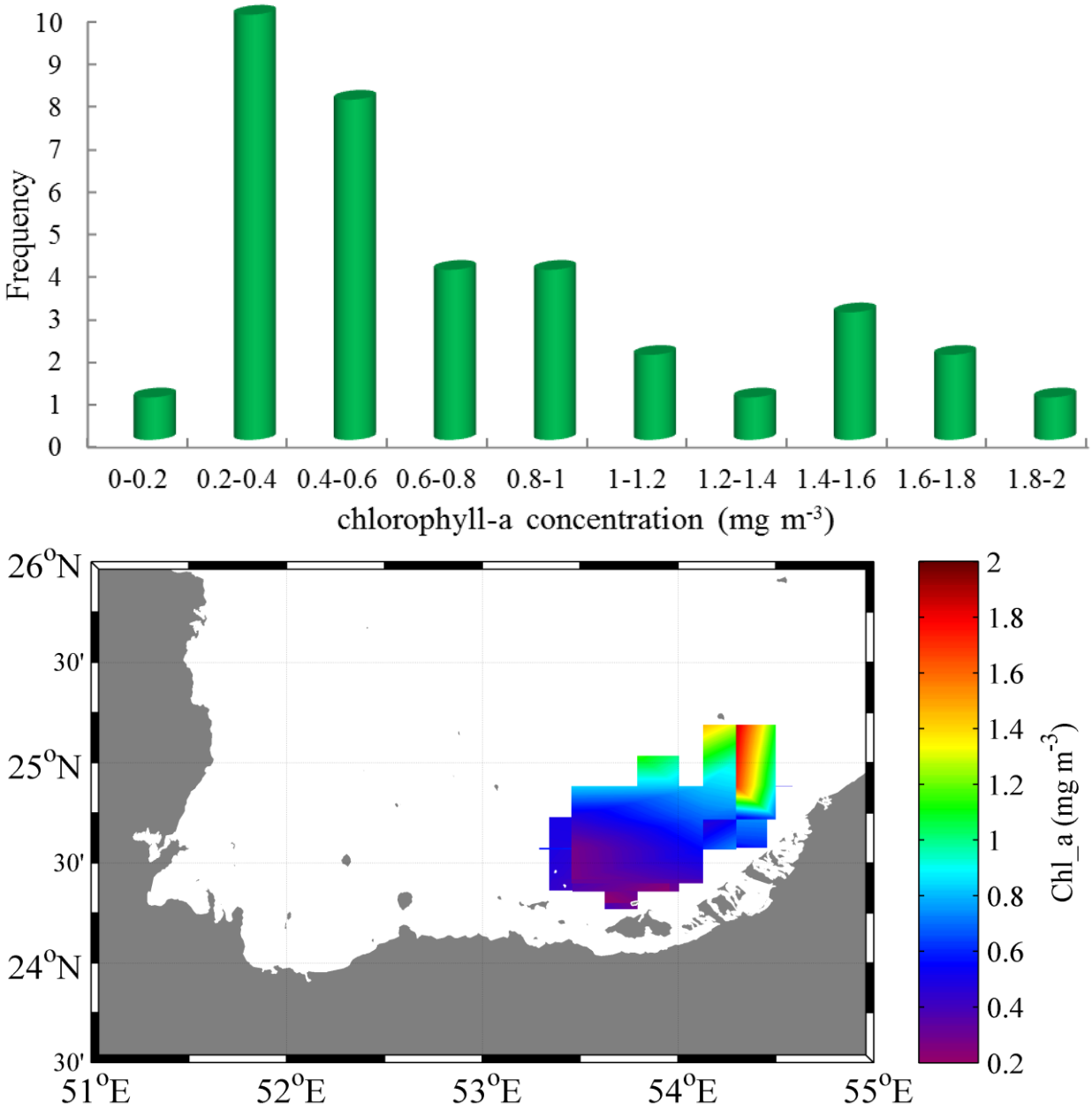

Figure 15:(a) Histogram of in situ measured chlorophyll-a. (b) Map showing the spatial distribution of in situ measured chlorophyll-a. A cubic interpolation method was used.

$$Chl = 2.31 * RI_1^{\,2} + 1.35 * RI_1 + 0.38$$

$$Chl = 2.19 * RI_2^{\,2} + 1.31 * RI_2 + 0.41$$

$$Chl = 0.11 * RI_3^{\,2} + 0.18 * RI_3 + 0.13$$

$$Chl = 0.087 * RI_4^{\,2} + 0.26 * RI_4 + 0.095$$

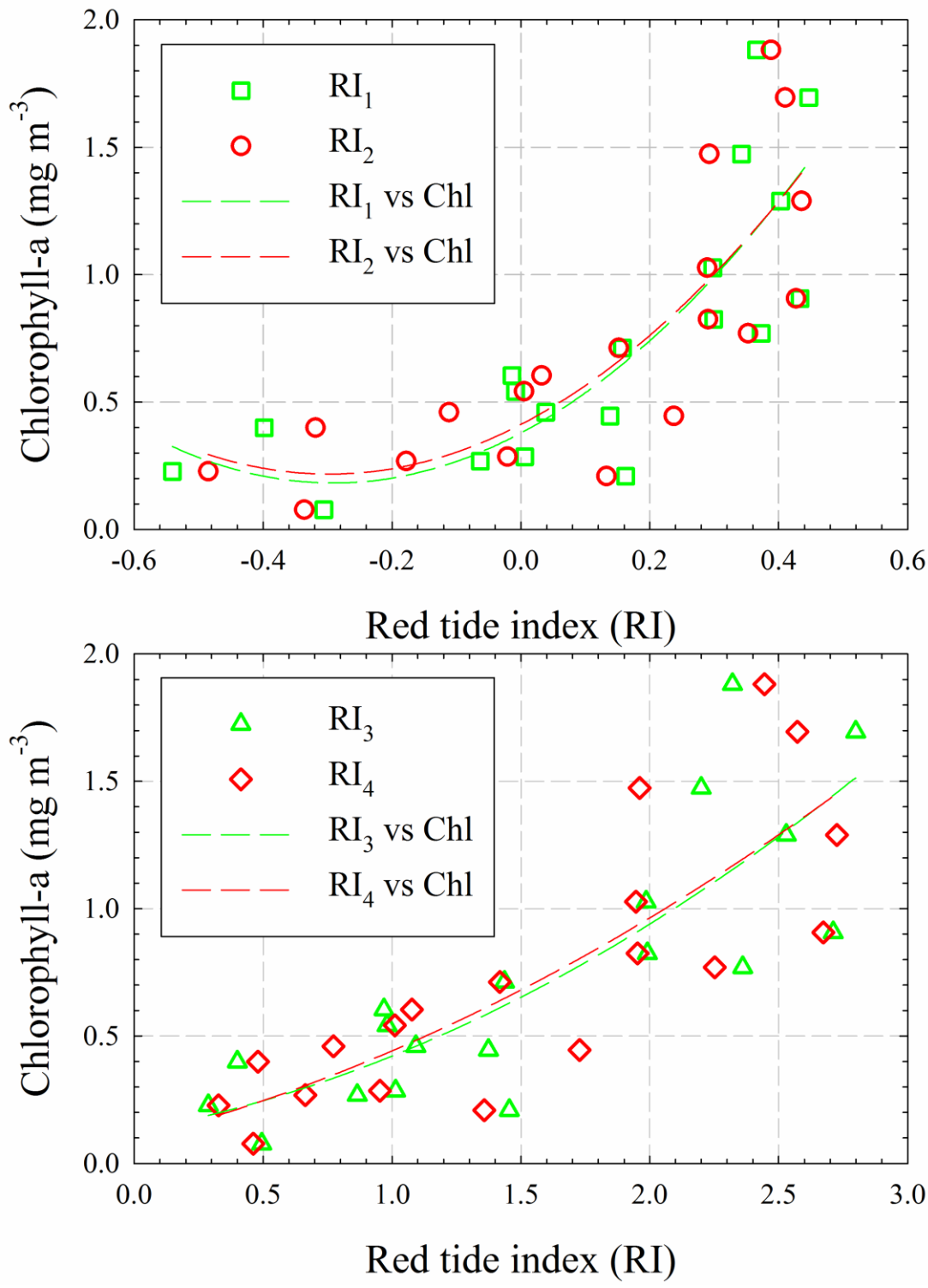

Figure 16: Relationship between different red tide indices and chlorophyll-a concentration from field surveys. The dashed lines indicate the best fits using quadratic functions.

However, the findings suggested that the quadratic formulation indicated superiority to other methods. Figure 17 shows the comparison between chlorophyll-a estimated from the discrete model using the validation dataset and measured from field surveys. The statistical results are summarized in table 7.

Table 7: Statistical results for the comparison between measured and estimated chlorophyll-a concentrations

Model	R^2	Mean ratio	Relative error (%)	RMSE (%)
RI_1	0.63	1.20	19.52	32.33
RI_2	0.62	1.18	17.56	28.28
RI_3	0.62	1.19	19.45	32.88
RI_4	0.61	1.17	16.56	29.55

The fourth model RI_4 appears to have the best performance as indicated by the lowest relative error and the lowest relative error, and by the mean ratio closest to 1,

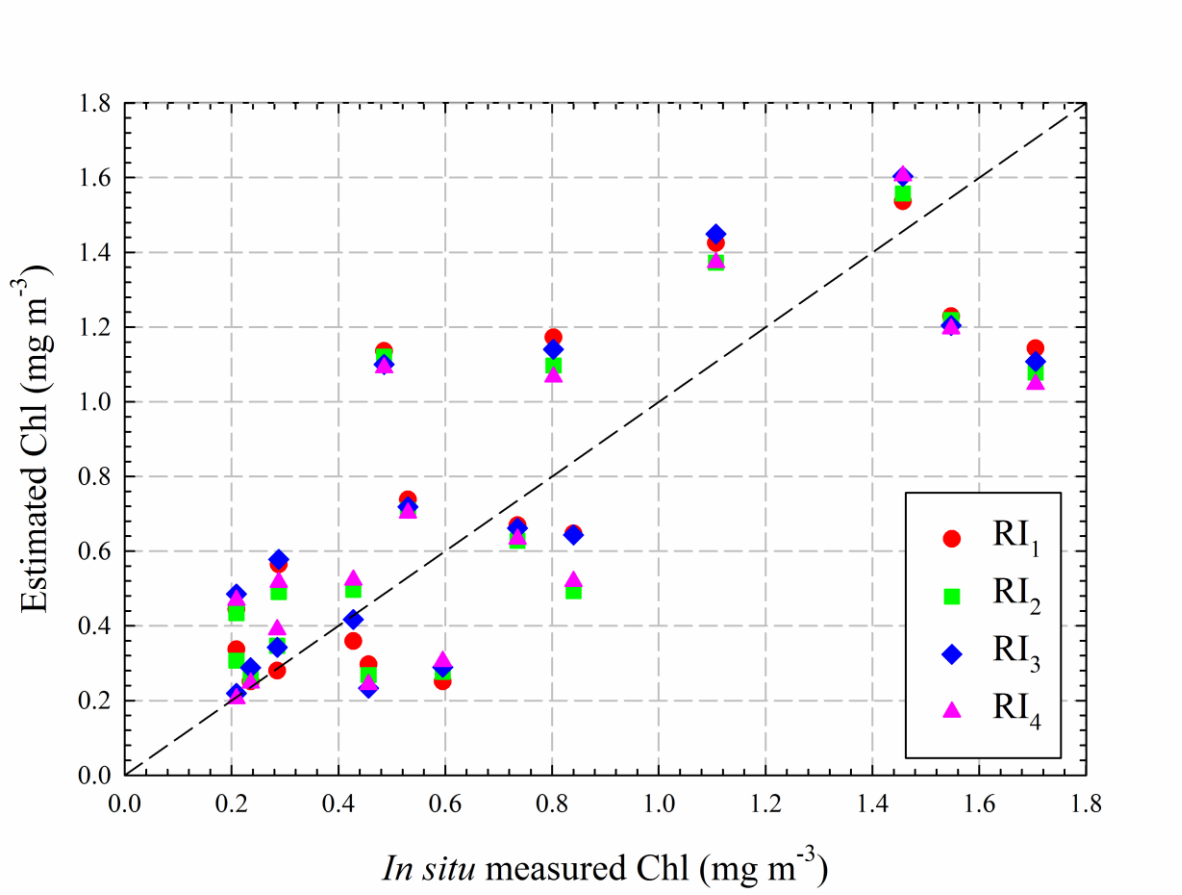

Figure 17: Comparison between in situ and estimated chlorophyll-a using the validation data set.

although the R^2 for RI_4 did not show remarkable superiority to others. Therefore, in this study, RI_4 will be utilized as an indicator of algal bloom. Hereafter RI will be used instead of RI_4.

4.3 Comparisons between RI and other indicators of algal bloom

As reported in previous studies [117] [118], different parameters have been used to indicate the occurrence of algal blooms, such as satellite derived chlorophyll-a maps and solar induced chlorophyll-a fluorescence. All of these methods have their own advantages and disadvantages. The operational chlorophyll-a product from satellite measurements is derived from an empirical blue-green band ratio algorithm. It was originally designed from case I waters where other components in the water column co-vary with phytoplankton. However, in optically complex case II waters, the empirical algorithm for chlorophyll fails, since the assumption based on which the empirical algorithm was established does not hold. Carder et al. (2003) noted that the

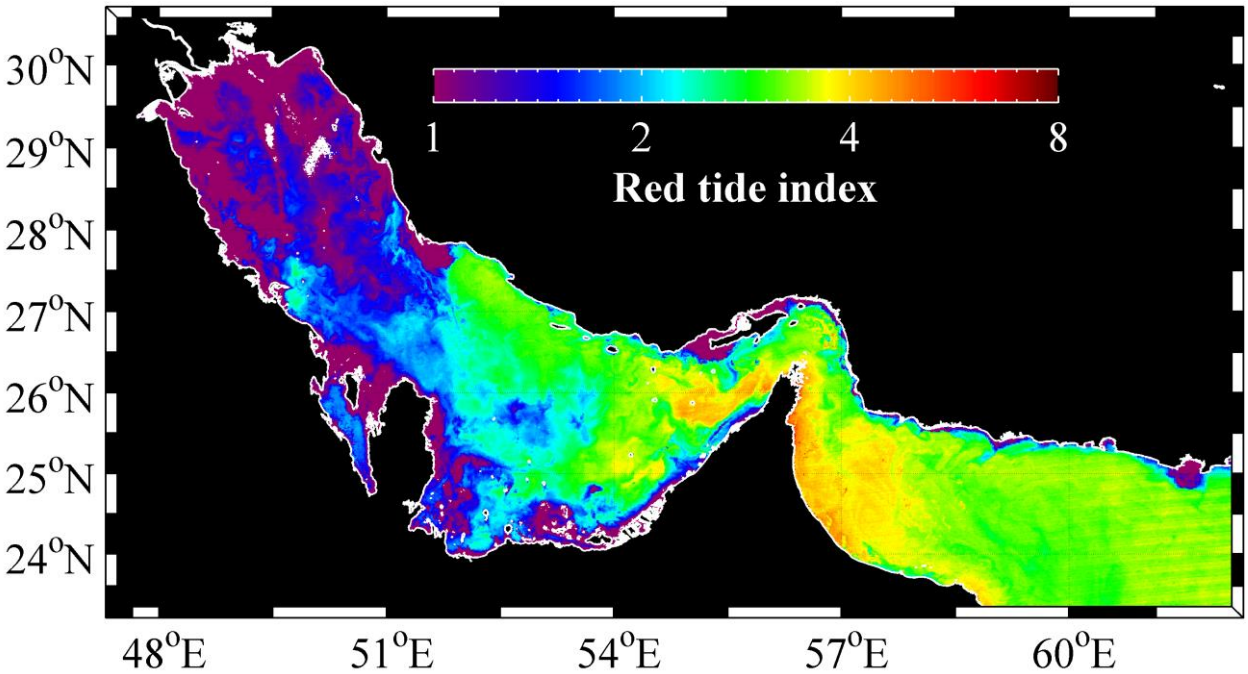

chlorophyll-a concentration might be underestimated during intensive bloom

Figure 18: Map of red tide index collected by MODIS/Aqua on December 23 2008 over the Arabian Gulf and the Sea of Oman.

fluorescence has been successfully used for bloom patch mapping, and it is sensitive to suspended sediment which can also lead to high signal in the red band where chlorophyll-a fluoresces. Furthermore, false alarms of algal bloom may happen due to the possible presence of submerged vegetation, such as sea-grass (Zhao et al., 2015).

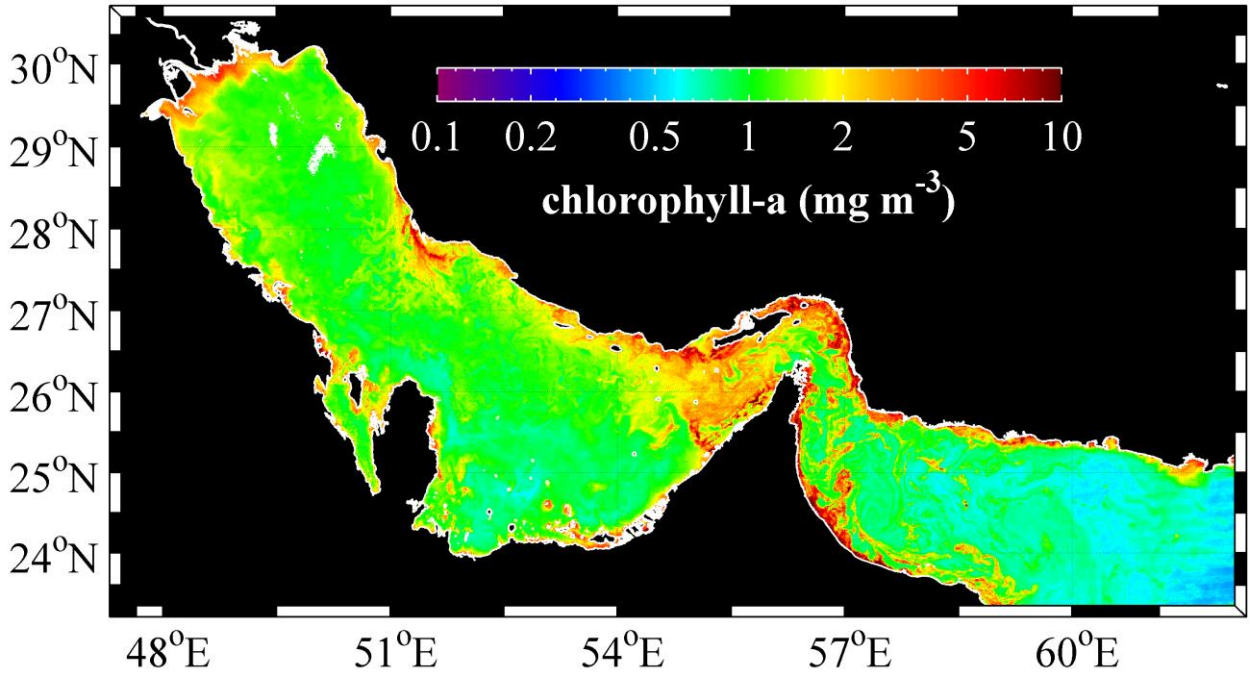

Figure 19: MODIS/Aqua derived chlorophyll-a map collected on December 23 2008 over the gulf using the default OC3M algorithm.

As an example, figures 18-20 compare RI, chlorophyll-a, and normalized fluorescence line height (nflh) for bloom mapping. The scene was collected by MODIS/Aqua on December 23 2008 when there was an extensive algal bloom event [118]. The RI map shows that the bloom extended from the east coast of Saudi Arabia, north of Qatar and south west of Iran, to the Sea of Oman. It appears that the bloom affected almost the whole west coast of UAE. However, in the chlorophyll-a map, the bloom patch cannot be separated from non-bloom waters except in the eastern Arabian Gulf. This could be caused by the global parameterization of the

default OC3M algorithm for MODIS sensor. On the other hand, the nflh map shows similar coverage of bloom to RI. However, for areas outlined with red circles in figure 20a, the high nflh values were probably caused by suspended sediment or shallow bottom as indicated by the bright color in the ERGB image. ERGB images have been suggested being integrated with nflh to identify bloom patches [117]. In contrast, RI shows low values in those areas and seems to be insensitive to suspended sediment and shallow bottom. Although bottom reflection mainly affects the R_{rs} spectra in the green wavebands, it seems that its effect was removed using the formulation of RI proposed in this study.

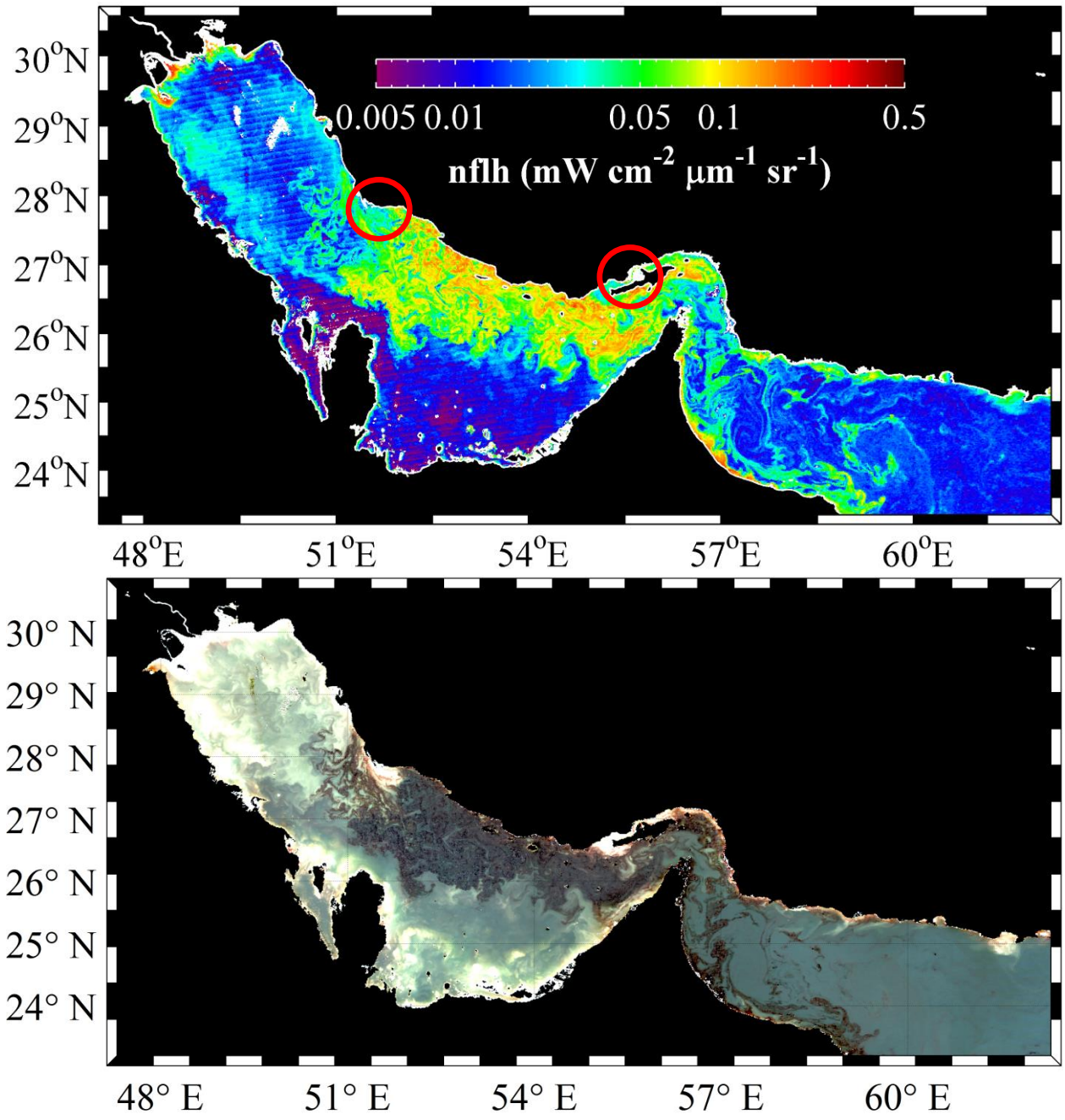

Figure 20:MODIS/Aqua derived normalized fluorescence line height (nflh) and enhanced Red-Green-Blue (ERGB) images collected on December 23 2008 over the gulf. High nflh and dark color in the ERGB image indicate occurrence of algal bloom.

4.4 Seasonal variations of RI in the gulf

Figure 21 shows the time series of monthly mean RI from 2002 to present over the whole Arabian Gulf. High RI values were found between late fall and early spring while low values were found in late spring and early fall. This shows good agreement

with findings reported by Nezlin et al. (2010). Using SeaWiFS data, they showed that chlorophyll-a was high in winter and low in summer. High chlorophyll-a in the winter was probably related to the decreased stratification of the water column. The nutrient-rich bottom water was swirled up by strong wind. Furthermore, surface cooling also contributed to the well mixing activities of the ocean circulation. Thus, phytoplankton growth was supported by the extra nutrients. Outbreaks of algal blooms may happen. While in the summer, the solar heating is very strong, and this leads to the strong stratification in the water column. Nutrient-rich bottom water is very difficult to be transported to the surface layer. However, there were exceptional cases. For example, the 2008 algal bloom event was first found in late August along the eastern coast of UAE. Zhao et al. (2014) proposed that the 2008 bloom event could be triggered by upwelling. In the summer, the southwest monsoon prevails in the region and it is favorable for upwelling.

For comparison, a satellite derived chlorophyll-a concentration using the default OC3M algorithm is also presented. The satellite derived chlorophyll-a shows a similar trend of variations to RI for chlorophyll-a < 2 mg m^{-3}. However, the patterns of variations of RI and satellite measured chlorophyll-a do not match well for chlorophyll-a > 2 mg m^{-3}. Regression analysis indicated that there was no significant correlation for this chlorophyll-a range. This is explainable. The correlation between RI and *in situ* chlorophyll-a was originally proposed for chlorophyll-a < 2 mg m^{-3}. On the other hand, we should bear in mind that there were uncertainties in satellite-derived chlorophyll-a concentrations due to several factors, such as atmospheric correction failure, and algorithm failure.

Both RI and satellite measured chlorophyll-a showed high productivity in 2003 and 2004 when extensive algal blooms were reported [119]. Between 2005 and 2007,

chlorophyll-a concentrations were generally less than 2 mg m^{-3} and there was no remarkable peak of RI. As reported by Zhao et al. (2014), an extensive algal bloom event started in late August 2008 and ended in late August 2009 in the gulf region. Satellite derived chlorophyll-a indicated significantly values as high as 3.5 mg m^{-3} in the winter of 2008. However, RI did not show corresponding high values. Between 2009 and 2015, the peaks of RI and chlorophyll-a matched well but with some exceptions, such as in the winter of 2010 and 2011.

4.5 Uncertainties of the RI

Although RI can delineate the general pattern of algal bloom, uncertainties still exist. As shown in figure 20, nflh and ERGB can show the bloom slicks very clearly. But the slick features cannot be separated from the background in the RI image. This is probably related to the model design. In extensive bloom conditions, L_w values are low in the blue region, while L_w increased in the red region where chlorophyll-a fluoresces and particulate backscattering increases.

Since RI was calculated using L_w, when satellite data are involved, satellite received signal contributed by aerosol must be removed. The operational atmospheric correction scheme assumes that the radiance in the near-infrared region is negligible, commonly referred to as 'black pixel assumption'. However, this scheme failed for optically complex coastal waters. As shown by Zhao et al. (2015), the default atmospheric correction method failed when extensive bloom conditions were encountered in 2008 in the Sea of Oman. Furthermore, the atmosphere over the Gulf region has high loads of dust with an estimated average flux of 6.385 g m^{-2} day^{-1} for an average of 33 days per year [120]. This heavy load of dust in the atmosphere has posed major challenges to the process of atmospheric correction. In SeaDAS, the

default thresholds of cloud albedo and aerosol optical depth at 865 nm (AOD_865) are 0.027 and 0.3, respectively. Any pixels with albedo > 0.027 or AOD_865 > 0.3 are masked during the processing from level 1 to level 2. Although the scientific community has given great efforts to this issue, to date, no scheme specifically designed for dust correction of ocean color data has been adopted into the mainstream satellite data processing. Therefore, regional atmospheric correction schemes are of great importance and must be developed for accurate application of ocean color products.

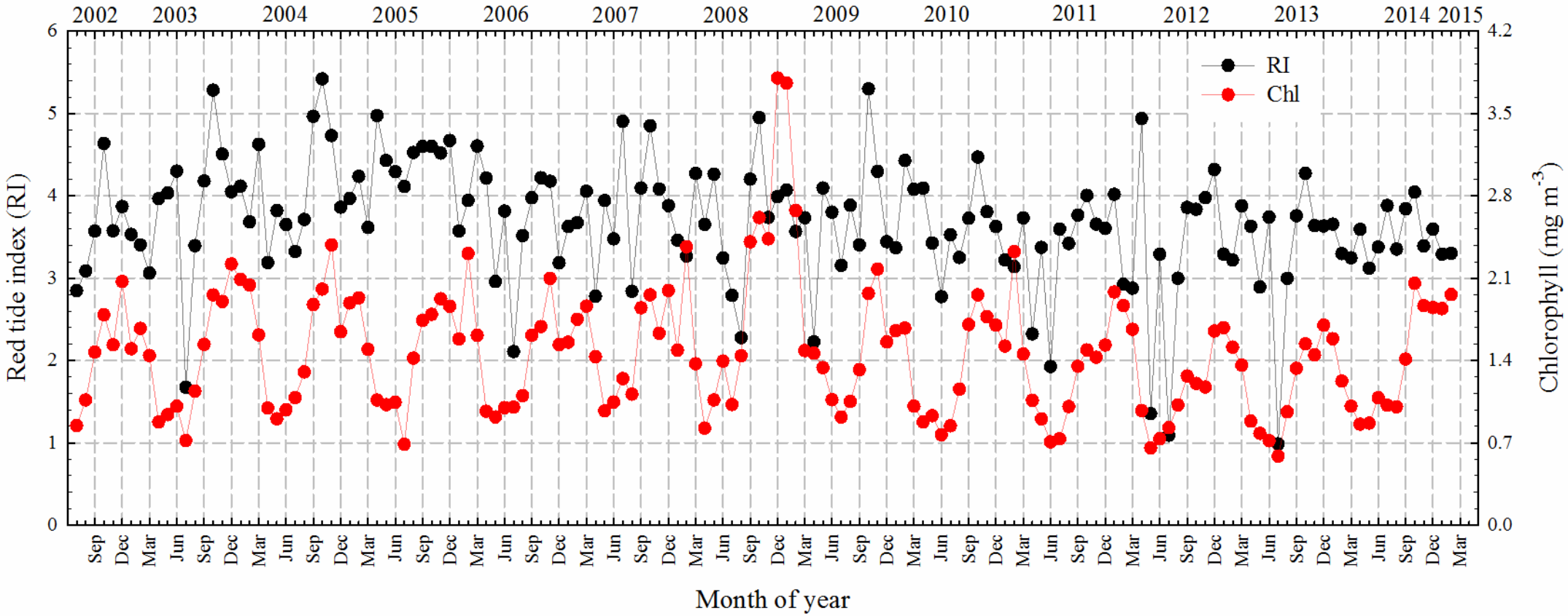

Figure 21: Times series of MODIS/Aqua derived RI from 2002 to 2015 over the whole gulf region. The satellite derived chlorophyll-a concentration using the operational band ratio algorithm is also plotted for comparison.

CHAPTER 5

Conclusion

Rapid detection of HABs has become increasingly important to mitigate the drawbacks, as the incidence of HABs has become more common. Satellite remote sensing has been widely used to detect HABs and the oceanographic environmental characteristics that favor the formation of HABs. Remote sensing is one of the methods to detect the outbreaks of any red tides event by using satellite observations. This approach is highly recommended as it gives high spatial and temporal coverage over large scales. Compared with traditional in situ point observations; include *in situ* ship-surveys and laboratory analysis; satellite remote sensing is considered as a promising technique for studying HABs.

Our field surveys showed that the highest chlorophyll-a concentration was in fall while the lowest in summer which consist with the literature result. On the other hand the spatial distribution showed opposite manner as the chlorophyll-a concentration increase from onshore to offshore owing to the terrestrial runoff in the region.

In this study, a regional index was developed by using different models using *in situ* data. The data that was used for algorithm development is 19 stations within the total 36 stations while the rest 17 stations were used for the algorithm validation using data independent. Four models were proposed, which plotted against chlorophyll-a

concentration using quadratic formulation to detect the best performance. A statistical test for the comparison between measured and estimated chlorophyll-a concentrations was also carried out to confirm that RI_4 is the best model. Therefore RI_4 was used as an indicator of algal blooms in this study. The new index that was developed in this study was compared with the other indicators of algal blooms such as satellite derived chlorophyll-a and FLH.

Times series of MODIS/Aqua derived RI from 2002 to 2015 over the whole gulf region was performed. The satellite derived chlorophyll-a concentration using the operational band ratio algorithm is also plotted for comparison. It showed a similar trend for chlorophyll-a < 2 mg m^{-3} while for chlorophyll-a > 2 mg m^{-3} was not matching. The present operational product from NASA showed that chlorophyll-a is sufficient and could be supported by the proposed red tide index in the Gulf. Our Masdar-based near real time satellite data processing system can output this index.

Recommendation

- Satellite imagery can provide a synoptic view of the marine environment over large temporal scales.
- With a times series of satellite measurements, the responses of the marine environment, such as coral reefs, sea grass to climate changes can be studied.
- The effects of desalination plants on the water quality in the gulf region can be tracked.
- Operational warning and forecasting system based on satellite observations are very helpful for marine resources protection and decision making in emergency situations, such as oil spills, and red tide.

References:

[1] P. M. Glibert, Anderson, D.M., Gentien, P., Graneli, E., Sellner, K.G.2005, " The global, complex phenomena of harmful algal blooms. Oceanography " vol. 18, 137–147.

[2] S. F. T. Wang, D. L.; He, F. L., 2008. , "Occurrences of harmful algal blooms (HABs) associated with ocean environments in the South China Sea.Hydrobiologia," vol. 596, 79-93.

[3] X. Lou and C. Hu, "Diurnal changes of a harmful algal bloom in the East China Sea: Observations from GOCI," *Remote Sensing of Environment,* vol. 140, pp. 562-572, 2014.

[4] M. O. Lee and J. K. Kim, "Characteristics of algal blooms in the southern coastal waters of Korea," *Mar Environ Res,* vol. 65, pp. 128-47, Mar 2008.

[5] R. F. Shipe, A. Leinweber, and N. Gruber, "Abiotic controls of potentially harmful algal blooms in Santa Monica Bay, California," *Continental Shelf Research,* vol. 28, pp. 2584-2593, 2008.

[6] A. J. Lewitus, R. A. Horner, D. A. Caron, E. Garcia-Mendoza, B. M. Hickey, M. Hunter, D. D. Huppert, R. M. Kudela, G. W. Langlois, J. L. Largier, E. J. Lessard, R. RaLonde, J. E. Jack Rensel, P. G. Strutton, V. L. Trainer, and J. F. Tweddle, "Harmful algal blooms along the North American west coast region: History, trends, causes, and impacts," *Harmful Algae,* vol. 19, pp. 133-159, 2012.

[7] M. L. Richlen, S. L. Morton, E. A. Jamali, A. Rajan, and D. M. Anderson, "The catastrophic 2008–2009 red tide in the Arabian gulf region, with observations on the identification and phylogeny of the fish-killing dinoflagellate Cochlodinium polykrikoides," *Harmful Algae,* vol. 9, pp. 163-172, 2010.

[8] D. V. Subba-Rao, Al-Yamani, F., 1998 "Phytoplankton ecology in the water between Shatt Al-Arab and the Straits of Hurmuz, Arabian Gulf: a review," *Plankton Biol. Ecol.,* vol. 45, 101–116.

[9] Y.-H. Ahn and P. Shanmugam, "Detecting the red tide algal blooms from satellite ocean color observations in optically complex Northeast-Asia Coastal waters," *Remote Sensing of Environment,* vol. 103, pp. 419-437, 2006.

[10] J. Zhao and H. Ghedira, "Monitoring red tide with satellite imagery and numerical models: A case study in the Arabian Gulf," *Mar Pollut Bull,* vol. 79, pp. 305-13, Feb 15 2014.

[11] S. Hamzehei, A. A. Bidokhti, M. S. Mortazavi, and A. Gheiby, "Red Tide Monitoring in the Persian Gulf and Gulf of Oman Using MODIS Sensor Data," *Technical Journal of Engineering and Applied Sciences,* vol. 2013-3-12/1100-1107, 2013.

[12] N. P. Nezlin, I. G. Polikarpov, F. Y. Al-Yamani, D. V. Subba Rao, and A. M. Ignatov, Satellite monitoring of climatic factors regulating phytoplankton variability in the Arabian (Persian) Gulf," *Journal of Marine Systems,* vol. 82, pp. 47-60, 2010.

[13] P. C. Chu and Y.-h. Kuo, "Detection of Red Tides in the Southwestern Florida Coastal Region Using Ocean Color Data," *Proceedings on MTS/IEEE OCEANS 10, Seattle, Washington, USA,,* September 20-23, 2010.

[14] P. Shanmugam, "A new bio-optical algorithm for the remote sensing of algal blooms in complex ocean waters," *Journal of Geophysical Research,* vol. 116, 2011.

[15] Jensen J.R. 2000. Remote sensing of the environment: An Earth Resource Perspective. Prentice Hall.

[16] Dere S., Günes T., Sivaci R .1998., Trends Journal of Botany, 22, 13 (1998).

[17] Gitelson A.,. Grits Y,. Etzion D. 2000. Optimal properties of Nannochloropsis sp and application to remote estimation of cell mass. Biotechnology Bioengineering 69, 516 .

[18] Herrring David. 1999. What are phytoplankton? NASA Earth observatory website.http://earthobservatory.nasa.gov/Features/Phytoplankton/phytoplankton_1999.pdf.

[19] Sathyendranath, S, Prieur, L, Morel, A . 1989. A three-component model of ocean color and its application to remote sensing of phytoplankton pigments in coastal waters. International Journal of Remote Sensing 10: pp. 1373-1394.

[20] Tassan, S 1994.Local algorithms using SeaWiFS data for the retrieval of phytoplankton, pigments, suspended sediment, and yellow substance in coastal waters. Applied Optics 33: pp. 2369-2377.

[21] Carona David A., Garneaua Marie-E`ve , Seuberta Erica , Meredith D.A. Howarda,b ,Lindsay Darjanya , Schnetzera Astrid, Cetinic´a Ivona, Gerry Filteauc, Laurid Phil, Jonesa Burton, Trusselle Shane. 2010. Harmful algae and their potential impacts on desalination operations off southern California. water research 44: 385–416.

[22] Andersen 1996. , Per. Design and implementation of some harmful algal monitoring systems. Paris: Unesco, 1996.

[23] Langlois, G., Smith, P., 2001. Phytoplankton. In: Karl, H.A., Chin, J.L., Ueber, E., Stauffer, P.H., Hendley III, J.W.(Eds.), Beyond the Golden Gate—Oceanography, Geology, Biology and Environmental Issues in the Gulf of the Farallones. U.S. Geological Survey Circular 1198, pp. 123–132.

[24] Al Shehhi Maryam R., Gherboudj Imen, Ghedira Hosni. 2014. An overview of historical harmful algae blooms outbreaks in the Arabian Seas. Marine Pollution Bulletin 86 314–324.

[25] Lindsey, R., Scott, M. and Simmon, R., 2010. What are phytoplankton?NASA's Earth Observatory. Available on http://earthobservatory.nasa.gov/Library/phytoplankton/.2010..

[26] Smayda, T.J., 1990. Novel and nuisance phytoplankton blooms in the sea: evidence for a global epidemic. In: Grane´li, E.,Gundstro¨m, B., Edler, L., Anderson, D.M. (Eds.), Toxic Marine Phytoplankton. Elsevier, New York, pp. 29–40.

[27] Hallegraeff, G.M., 1993. A review of harmful algal blooms and their apparent global increase. Phycologia 32 (2), 79–99.

[28] Hallegraeff, G.M., 2003. Harmful algal blooms: a global overview. In: Hallegraeff, G.M., Anderson, D.M., Cembella, A.D. (Eds.), Manual on Harmful Marine Microalgae. Monographs on Oceanographic Methodology. UNESCO Publishing, Paris pp. 25–49.

[29] Anderson, D.M., Glibert, P.M., Burkholder, J.M., 2002. Harmful algal bloomsandeutrophication: nutrient sources, composition,and consequences. Estuaries 25 (4B), 704–726.

[30] Glibert, P.M., Anderson, D.M., Gentien, P., Graneli, E., Sellner, K.G., 2005. The global, complex phenomena of harmful algal blooms. Oceanography 18 (2), 137–147.

[31] D'Silva, M.S., Anil, A.C., Naik, R.K., D'Costa, P.M., 2012. Algal blooms: a perspective from the coasts of India. Nat. Hazard 63, vol. 63. 1225–1253.

[32] Padmakumar, K.B., Menon, N.R., Sanjeevan, V.N., 2012. Is occurrence of harmful algal blooms in the exclusive economic zone of India on the rise? Int. J. Oceanogr. 2012. http://dx.doi.org/10.1155/2012/263946..

[33] Thangaraja Muthian, Al-Aisry Ahmed and Al-Kharusi Lubna. 2007. Harmful algal blooms and their impacts in the middle and outer ROPME sea area. International Journal of Oceans and Oceanography. ISSN 0973-2667 Volume 2, pp. 85–98.

[34] Richlen, M.L., Morton, S.L., Jamali, E.A., Rajan, A., Anderson, D.M., 2010. The catastrophic 2008–2009 red tide in the Arabian gulf region, with observations on the identification and phylogeny of the fish-killing dinoflagellate Cochlodinium polykrikoides. Harmful Algae 9, 163–172. http://dx.doi.org/ 10.1016/j.hal.2009.08.013.

[35] Saeedi, H., Kamrani, E., Matsuoka, K., 2011. Catastrophic impact of red tides of Cochlodinium polykrikoides on the Razor Clam Solen dactylus in Coastal Waters of the Northern Persian Gulf. J. Persian Gulf 2, 13–20.

[36] Glibert, P.M., Landsberg, J.H., Evans, J.J., Al-Sawari, M.A., Faraj, M., Al-Jarallah, M.A., Haywood, A., Ibrahem, S., Klesius, P., Powell, K., Shoemaker, C., 2002. A fish kill of massive proportion in Kuwait Bay, Arabian Gulf, 2001: the roles of bacterial disease, harmful algae, and eutrophication. Harmful Algae 1, 215–231.

[37] Heil, C.A., Glibert, P.M., Al-Sarawl, M.A., Faraj, M., Behbehani, M., Husain, M., 2001. First record of a fish-killing Gymnodinium sp bloom in Kuwait Bay, Arabian Sea: chronology and potential causes. Mar. Ecol. Ser. 214, 15–23.

[38] Subba Rao, D.V., Al-Hassan, J.M., Al-Yamani, F., Al-Rafaie, K., Ismail, W., Nageswara Rao, C.V., and Al-Hassan, A. 2003," Elusive red tides in Kuwait coastal waters", Harmful Algae News, 24:10-13, The IOC of UNESCO.

[39] Al-Yamani, F., J. Bishop, W. Ismaeil, K. Al-Rifaie, A. Al-Yaqout, T. Al-Salld, A. Kwarteng, A. AI-Ghadban, L. Al-Omran & C. Sheppard. 1997. Assessment of the Effects of the Shatt Al-Arab's Altered Discharge Regimes on the Ecology ofthe Northern Arabian Gulf. Final Report-FM006K. Kuwait Institute for Sci entific Research. Kuwait, 258 pp.

[40] Al-Ansi, M.A., Abdel-Moati, M.A.R., Al-Ansari, I.S., 2002. Causes of fish mortality along the Qatari waters (Arabian Gulf). Int. J. Environ. Stud. 59, 59–71.

[41] Al-Busaidi, S.S., Al-Rashdi, K.M., Al-Gheilani, H.M., Amer, S., 2008. Hydrographical observations during a red tide with fish mortalities at Masirah Island, Oman. J. Agric. Mar. Sci. 13, 63–72.

[42] Morton, S.L., Faust, M.A., Fairey, E.I., Moeller, P.D.R., 2002. Morphology and toxicology of Prorocentrum arabianum sp. nov.,(dinophyceae) a toxic planktonic dinoflagellate from the Gulf of Oman, Arabian Sea. Harmful Algae 1, 393–400. http://dx.doi.org/10.1016/S1568-9883(02)00047-1..

[43] Krishnan, A.A., Krishnakumar, P.K., Rajagopalan, M., 2007. Trichodesmium erythraeum (Ehrenberg) bloom along the southwest coast of India (Arabian Sea) and its impact on trace metal concentrations in seawater. Estuarine, Coastal and Shelf Science., Issues 3–4. 71:641–646.

[44] Joseph, T., Shaiju, P., Laluraj, C.M., Balachandran, K.K., Nair, M., George, R., Nair, K.K., Sahayak, S., Prabhakaran, M.P., 2008. Nutrient environment of red tide-infested waters off south-west coast of India. Environ. Monit. Assess. 143, 355–361. .

[45] Matondkar S G P, Bhat S R, Dwivedi R M, Nayak S R. 2004. Indian Satellite IRS-P4 (OCEANSAT) monitoring algal blooms in the Arabian Sea. Harmful Algae News, 26 : 4-5.

[46] Madhupratap, M., Sawant, S., Gauns, M., 2000. A first report on a bloom of the marine prymnesiophycean, Phaeocystis globosa from the Arabian Sea. Oceanol. Acta 23, 83–90.

[47] Chaghtai, F., Saifullah, S.M., 2001. Harmful algal bloom (HAB) organisms of the north Arabian sea bordering Pakistan. Pakistan J. Bot. 33, 69–75.

[48] Padmakumar, K.B., Menon, N.R., Sanjeevan, V.N., 2012. Is occurrence of harmful algal blooms in the exclusive economic zone of India on the rise? Int. J. Oceanogr. 2012. http://dx.doi.org/10.1155/2012/263946..

[49] Saifullah, S.M., 1979. Occurrence of dinoflagellates and distribution of chlorophyll A on Pakistan shelf. In: Taylor, D.L., Seliger, H.H. (Eds.), Toxic Dinoflagellate Blooms. Elsevier, North Holland, New York, pp. 203–208.
[50] D'Silva, M.S., Anil, A.C., Naik, R.K., D'Costa, P.M., 2012. Algal blooms: a perspective from the coasts of India. Nat. Hazard 63, vol. 63. 1225–1253.
[51] Jewett, E.B., Lopez, C.B., Dortch, Q., and Etheridge, S.M. 2007. National Assessment of Efforts to predict and Respond to Harmful Algal Blooms in U.S. Waters. Interim Report. Interagency Working Group on Harmful Algal Blooms, Hypoxia, and Human Health of the Joint Subcommittee on Ocean Science and Technology. Washington, DC.
[52] Anderson, D. M. (2007). The Ecology and Oceanography of Harmful Algal Blooms: Multidisciplinary Approaches to Research and Management. UNESCO.
[53] Hanieh Saeedi, Ehsan Kamrani, Kazumi Matsuoka. 2011. Catastrophic Impact of Red Tides of Cochlodinium polykrikoides on the Razor Clam Solen dactylus in Coastal Waters of the Northern Persian Gulf. Journal of the Persian Gulf (Marine Science)/Vol. 2/No. 6//7/13-20.
[54] Menon, S. (2009, June 14). Fishing Industry in Eastern Areas Badly Hit by Red Tide . Retrieved July 22, 2009, from Gulf News: http://www.gulfnews.com/nation/Environment/10322625.html .
[55] Foster KA, Foster G, Tourenq C, Shurique MK (2011) Shifts in coral community structures following cyclone and red tide disturbances within the Gulf of Oman (United Arab Emirates). Mar Biol 158:955–968.
[56] Heil, C.A., Glibert, P.M., Al-Sarawl, M.A., Faraj, M., Behbehani, M., Husain, M., 2001. First record of a fish-killing Gymnodinium sp bloom in Kuwait Bay, Arabian Sea: chronology and potential causes. Mar. Ecol. Ser. 214, 15–23.
[57] Cloern, J.E., 1999. The relative importance of light and nutrient limitation of phytoplankton growth: a simple index of coastal ecosystem sensitivity to nutrient enrichment. Aquat. Ecol. 33, 3–16. http://dx.doi.org/10.1023/ A:1009952125558.
[58] Houser, J.N., Richardson, W.B., 2010. Nitrogen and phosphorus in the Upper Mississippi River: transport, processing, and effects on the river ecosystem. Hydrobiologia 640, 71–88. http://dx.doi.org/10.1007/s10750-009-0067-4..
[59] Al-sahli, M.M., 2007. Estimating Chlorophyll Concentrations of Kuwait's Coastal Environment Using SeaWiFS and MODIS Satellite Data. ProQuest.
[60] McConnell, M, 2002. GloBallast Legislative Review –Final Report. GloBallast Monograph Series No.1. IMO London.
[61] Al Qubaisi, B. S. 2006. A Study of Factors Influencing the Occurrence of Algae Bloom (HAB) Along the Abu Dhabi Coast, UAE. United Arab Emirates University (p. 98). Abu Dhabi: Environment Agency- Abu Dhabi.
[62] Husar, R.B., Prospero, J.M., Stowe, L.L., 1997. Characterization of tropospheric aerosols over the oceans with the NOAA advanced very high resolution radiometer optical thickness operational product. Journal of Geophysical Research—Atmospheres 102 (D14), 16889–16909.
[63] Haake. B and Ittekkot, V. 1990:Die wind-getribenc "biologische Pumpe and Kohlenstoffentzug im Ozean :Naturwissenschften. 77, 75-79 p.
[64] Duce, R.A., Tindale, N.W., 1991. Atmospheric transport of iron and its deposition in the ocean. Limnology and Oceanography 36 (8), 1715–1726.
[65] Martin, J.H., Coale, K.H., Johnson, K.S., Fitzwater, S.E., Gordon, R.M., Tanner, S.J., Hunter, C.N., Elrod, V.A., Nowicki, J.L., Coley, T.L., Barber, R.T., Lindley, S., Watson, A.J., Van Scoy, K., Law, C.S., Liddlcoat, M.I., Ling, R., Stanton, T., Stockel, J., Collins, C., Anderson, A., Bidigare, R.R., Ondrusek, M., Latasa, M., Millero, F.J., Lee, K., Yao, W., Zhang, J.Z., Friederich, G.E., Sakamoto, C., Chavez, F.P., Buck, K.R., Kolber, Z.,

Greene, R., Falkowski, P.G., Chisholm, S.W., Hoge, F.E., Swift, R., Yungel, J., Turner, S., Nightingale, P., Hatton, A., Liss, P., Tindale, N.W., 1994. Testing the iron hypothesis in ecosystems of the equatorial Pacific Ocean. Nature 371 (6493), 123–129.

[66] deBaar, H.J.W., deJong, J.T.M., Bakker, D.C.E., Loscher, B.M., Veth, C., Bathmann, U., Smetacek, V., 1995. Importance of iron for plankton blooms and carbon dioxide drawdown in the Southern Ocean. Nature 373, 412–415.

[67] Jickells, T.D., An, Z.S., Andersen, K.K., Baker, A.R., Bergametti, G., Brooks, N., Cao, J.J., Boyd, P.W., Duce, R.A., Hunter, K.A., Kawahata, H., Kubilay, N., laRoche, J., Liss, P.S.,Mahowald, N., Prospero, J.M., Ridgwell, A.J., Tegen, I., Torres, R., 2005. Global iron connections between desert dust, ocean biogeochemistry, and climate. Science 308 (5718), 67–71.

[68] Mahowald, N.M., Baker, A.R., Bergametti, G., Brooks, N., Duce, R.A., Jickells, T.D., Kubilay, N., Prospero, J.M., Tegen, I., 2005. Atmospheric global dust cycle and iron inputs to the ocean. Global Biogeochemical Cycles 19 (4), CB4025.

[69] Nezlin Nikolay P., Polikarpov Igor G., Al-Yamani Faiza Y. , Subba Rao D.V. Ignatov, Alexander M. 2010. Satellite monitoring of climatic factors regulating phytoplankton variability in the Arabian (Persian) Gulf. Journal of Marine Systems 82 47–60.

[70] Subba Rao, D.V., and F. Al-Yamani, A.Lennox, Y.Pan and T.F.O. Al said. 1999. Biomass and production characteristics of the first red tide noticed in Kuwait Bay, Arabian Gulf. J. J. Plankton Res. 21 (4): 805-810.

[71] Berger W. H. and Wefer G. 1991. Productivity of the glacial ocean: Discussion of the iron hypothesis. Global consequences: Past and future. Limnol. Oceanogr., 36(8), 1991, 1899-1918.

[72] Brewer, P.G., Dyrssen, D., 1985. Chemical oceanography of the Persian Gulf. Progress in Oceanography 14 (1–4), 41–55.

[73] Reynolds, M. 1993, “Physical oceanography of the Gulf, Strait of Hormuz, and the Gulf of Oman: Results from the Mt. Mitchell expedition”, Mar. Pollut. Bull., 27, pp. 35-59.

[74] Swift, S.A., Bower, A.S., 2003. Formation and circulation of dense water in the Persian/Arabian G Mishra S., and Mishra D.R. A novel remote sensing algorithm to quantify phycocyanin in cyanobacterial algal blooms. Environmental Research Letters, 2014, 9, 114003.

[75] John, V.C., 1992. Circulation and mixing processes and their effect on pollution distribution in the western Arabian Gulf. Applied Ocean Research, 14(1): 59-64.

[76] Abaychi, J. K.; Darmoian, S. A. and DouAbul, A. A. Z. (1988). The Shatt Al-Arab river : A nutrient salt and organic source to the Arabian Gulf. Hydrobiologia, 166: 271-224.

[77] Advisory 2009. MARINE SAFETY ADVISORY NO. 49-09. Reference: MEPC 59/INF.3.

[78] Raaymakers, S. 2002.The Ballast Water Problem: Global Ecological, Economic and Human Health Impacts. RECSO / IMO Joint Seminar on Tanker Ballast Water Management & Technologies. Dubai.

[79] Carlton, J.T., Geller, J.B., 1993. Ecological roulette: the global transport of nonindigenous marine organisms. Science 261, 78–82.

[80] Hallegraeff, G., 1998. Transport of toxic dinoflagellates via ships’ ballast water: bioeconomic risk assessment and efficacy of possible ballast water management strategies. Mar. Ecol. Prog. Ser. 168, 297–309.

[81] Palomar Pilar and Losada I. J. 2009. Impacts of Brine Discharge on the Marine Environment. Modelling as a Predictive Tool. Desalination, Trends and Technologies. 279-310.

[82] Al-Karaghouli Ali A. and Kazmerski L.L. 2011. Renewable Energy Opportunities in Water Desalination. Golden, Colorado, 80401, USA: National Renewable Energy Laboratory (NREL).
[83] CORDIS Database; 2006.
[84] IDA (2008): IDA Worldwide Desalting Plant Inventory, No. 20 in MS Excel format, Media Analytics Ltd., Oxford, UK.
[85] Bleninger, T. Niepelt A., G.H. Jirka S. Lattemann. A. Purnama & H.H. Al-Barwani. R.L. Doneker .2010. Environmental hydraulics framework of the design of discharges from desalination plants. Environmental Hydraulics – Christodoulou & Stamou (eds). Taylor & Francis Group, London, ISBN 978-0-415-58475-3.
[86] Dawoud Mohamed A and Al Mulla Mohamed M. 2012. Environmental Impacts of Seawater Desalination: Arabian Gulf Case Study. International Journal of Environment and Sustainability. ISSN 1927-9566 | Vol. 1 No. 3, pp. 22-37.
[87] Berktay, A., 2011. Environmental approach and influence of red tide to desalination process in the Middle East region. Int. J. Chem. Environ. Eng. 2, 183–188.
[88] R. Saidur, E. T. Elcevvadi, S. Mekhilef, A. Safari, and H. A. Mohammed, "An overview of different distillation methods for small scale applications," *Renewable and Sustainable Energy Reviews,* vol. 15, pp. 4756-4764, 2011.
[89] H. J. Krishna, "Introduction to Desalination Technologies.
[90] L. F. Greenlee, D. F. Lawler, B. D. Freeman, B. Marrot, and P. Moulin, "Reverse osmosis desalination: water sources, technology, and today's challenges," *Water Res,* vol. 43, pp. 2317-48, May 2009.
[91] Campbell, R.L. and Jones, A.T. (2005). Appropriate disposal of effluent from coastal desalination facilities. Desalination, 182, 365-372
[92] Preston, A., Zhao, G and Kavanagh, K.B. 2007. Dispersion modeling study: Gorgon Project-Barrow Island RO Plant Sea water Intake and Reject Brine Outfall. Flow Science.
[93] Tularam G. A and Ilahee M. 2007. Environmental concerns of desalinating sea water using reverse osmosis. Journal of Environmental Monitoring, 9, 805-813.
[94] Hashim A and Hajjaj M . 2005. Impact of desalination plants fluid effluents on the integrity of sea water , with the Arabian Gulf in perspective. Desalination , 182, 373-393..
[95] Latterman, S. and Hopner, T. 2008 . Environmental impact of impact assessment of sea water desalination. Desalination, 220, 1-15.
[96] Sadhwani J. Jaime, Veza Jose M., Santana Carmelo.2005. Case studies on environmental impact of seawater desalination. Desalination 185 1–8.
[97] Hopner, T. and Windelberg, J. 1996. Elements of environmental impact studies on coastal desalination plants. Desalination, 108, 11-18.
[98] Gacia, E.; Invers, O.; Ballesteros, E.; Manzanera M. & Romero, J. (2007). The impact of the brine from a desalination plant on a shallow seagrass (Posidonia oceanica) meadow. Estuarine, Coastal and Shelf Science, vol 72, Issue 4, pp.579-590.
[99] Einav .R and Lokiec F. 2003. Environmental aspects of a desalination plant in Ashkelon. Desalination, 156, 79-85.
[100] Reichelt-Brushett, A.J and Harrison P.L .2005. The effect of selected trace metals on the fertilization success of several scleractinian coral species. Coral Reefs, 24, 524-534.
[101] RPS.2009. Effects of a desalination plant discharge on the marine environment of barrow island. Report No: N09504.
[102] Gude Veera Gnaneswar, Nirmalakhandan Nagamany, Shuguang Deng. 2010.Renewable and sustainable approaches for desalination. Renewable and Sustainable Energy Reviews. 14 : 2641–2654.

[103] Berger L.R. little B. 1980. Effect of microfouling on heat transfer efficiency , 5th International congress on Marine Corrosion and fouling , Marine Biology Spain 1980 , pp 139-154.
[104] Gijsbertsen-Abrahamse, A.J., Schmidt, W., Chorus, I., Heijman, S.G.J.,2006. Removal of cyanotoxins by ultrafiltration and nanofiltration. Journal of Membrane Science 276 (1–2), 252–259.
[105] Lee, J., Walker, H.W., 2006. Effect of process variables and natural organic matter on removal of microcystin-LR by PAC-UF. Environmental Science and Technology 40 (23), 7336–7342.
[106] Reiss, C.R., Robert, C., Owen, C., Taylor, J.S., 2006. Control of MIB, geosmin and TON by membrane systems. Journal of Water Supply: Research and Technology – AQUA 55 (2), 95–108.
[107] WDR, 2008. Red tides close desal plants. In: T. Pankrantz (Ed.), Water Desalination Report, vol. 44, Houston, TX.
[108] Nazzal, N., 2009. 'Red tide' shuts desalination plant, Gulf News, Dubai, UAE, 3 March 2009. Available from http://archive.gulfnews.com/indepth/redtide/more_stories/10297763.html..
[109] D. M. Anderson and S. McCarthy, "Red Tides and Harmful Algal Blooms: Impacts on Desalination Operations," *Under the Patronage of HE Mohammed Al Mahrouqi Chairman of Oman PAEW,* vol. organized by the Middle East Desalination Research Center, National Center of Excellence, February 8-9, 2012.
[110] M. V. Laycock, D. M. Anderson, J. Naar, A. Goodman, D. J. Easy, M. A. Donovan, A. Li, M. A. Quilliam, E. Al Jamali, and R. Alshihi, "Laboratory desalination experiments with some algal toxins," *Desalination,* vol. 293, pp. 1-6, 2012.
[111] M. Wilf and C. Bartels, "Optimization of seawater RO systems design," *Desalination,* vol. 173, pp. 1-12, 2005.
[112] D. A. Caron, M. E. Garneau, E. Seubert, M. D. Howard, L. Darjany, A. Schnetzer, I. Cetinic, G. Filteau, P. Lauri, B. Jones, and S. Trussell, "Harmful algae and their potential impacts on desalination operations off southern California," *Water Res,* vol. 44, pp. 385-416, Jan 2010.
[113] Z. W. Wang, Zhichao Yin, Xing Tian, Lumei, "Membrane fouling in a submerged membrane bioreactor (MBR) under sub-critical flux operation: Membrane foulant and gel layer characterization," *Journal of Membrane Science,* vol. 325, pp. 238-244, 2008.
[114] F. C. Meng, S. R.Drews, A.Kraume, M.Shin, H. S.Yang, F., "Recent advances in membrane bioreactors (MBRs): membrane fouling and membrane material," *Water Res,* vol. 43, pp. 1489-512, Apr 2009.
[115] Y. Kim, Y. Byun, Y. Kim, and Y. Eo, "Detection of Cochlodinium polykrikoides red tide based on two-stage filtering using MODIS data," *Desalination,* vol. 249, pp. 1171-1179, 2009.
[116] Mishra S., and Mishra D.R.2014. A novel remote sensing algorithm to quantify phycocyanin in cyanobacterial algal blooms. Environmental Research Letters, 2014, 9, 114003.
[117] Zhao J., Ghedira H. 2014. Monitoring red tide with satellite imagery and numerical models: A case study in the Arabian Gulf. 2014. Marine Pollution Bulletin, 79, 305-313.
[118] Zhao J., Temimi M., Ghedira H. 2015. Characterization of harmful algal blooms (HABs) in the Arabian Gulf and the Sea of Oman using MERIS fluorescence data. 2015. ISPRS Journal of Photogrammetry and Remote Sensing, 101, 125-136.

[119] Gomes, H.doR., Goes, J.I., Matondkar, S.G.P., Parab, S.G., Al-Azri, A.R.N., Thoppil, P.G., 2008. Blooms of Noctiluca miliaris in the Arabian Sea-An in situ and satellite study. Deep-Sea Res. I 55, 751–765.

[120] W. Hamza, M. R. Enan, H. Al-Hassini, J.-B. Stuut, and D. de-Beer, “Dust storms over the Arabian Gulf: a possible indicators of climate changes consequences,” Aquat. Ecosyst. Health Manage. 14(3), 260–268 (2011).